Journal
of
The Franklin Institute
Devoted to Science and the Mechanic Arts

Vol. 246 OCTOBER, 1948 No. 4

RESEARCH WORK OF THE FRANKLIN INSTITUTE DURING WORLD WAR II ON AIRBORNE FIRE CONTROL APPARATUS.*

BY

RALPH H. McCLARREN.[1]

From 1824, when The Franklin Institute was founded, until today the Institute has participated actively in the advances of industry and science. Its past work in meteorology, boiler research, screw thread standardization, patent activities and other technical pursuits is known widely. But the increase in research and development done by the Institute during the war could not be made public until now. Security restrictions prevented such publicity. Indeed, much of the present work of the Laboratories is still held from publication by the security regulations.

However, some of the instruments developed during the war have been unclassified since the end of the war, and now it is possible to write of these instruments and to explain why they were vital to the victory.

The scientific and research investigations conducted at the Institute during World War II pertained, among other fields, to development of airborne fire control apparatus for military aviation. While the basis of a laboratory staff was assembled for this work, the Laboratories for Research and Development were not officially designated as a Department activity of The Franklin Institute until after the war. The original war contract with the Office of Scientific Research and Development (OEMsr-330) was negotiated in February 1942 and the technical work under this contract was supervised by Section 7.2 of the National

* Talk presented at a Joint Meeting of The Franklin Institute and the Instruments and Measurements Group of the American Institute of Electrical Engineers, January 7, 1948; released for publication by the Bureau of Ordnance, Navy Department.

[1] Director, Electronics and Instruments Division, The Franklin Institute Laboratories for Research and Development, Philadelphia, Penna.

(Note—The Franklin Institute is not responsible for the statements and opinions advanced by contributors in the JOURNAL.)

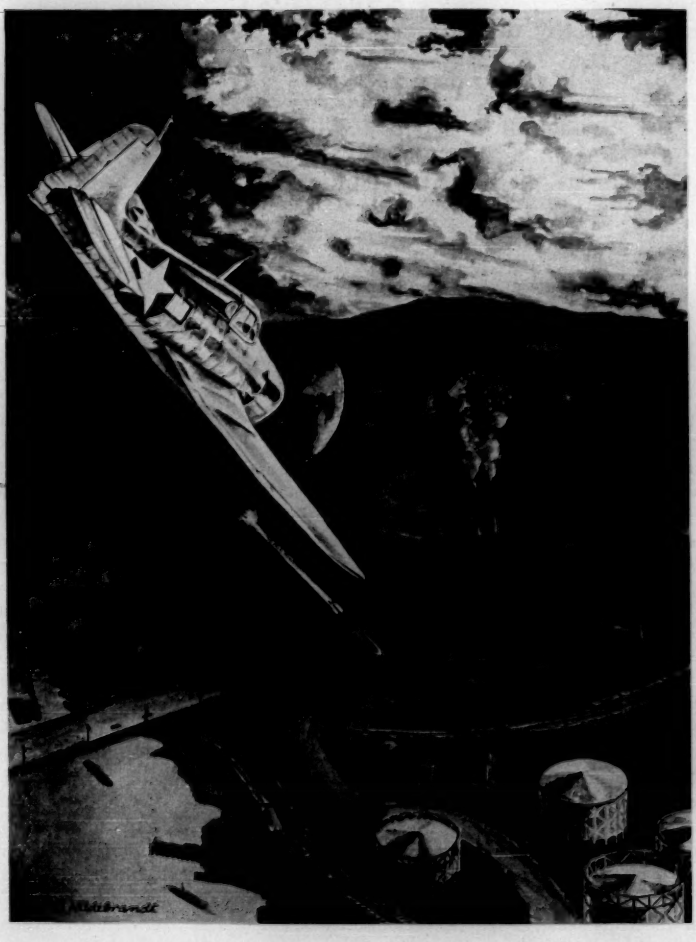

Defense Research Committee. Projects undertaken concerned the analysis, development, design, and construction of instruments, computers, and sighting systems for directing the fire of torpedoes, bombs, bullets, and rockets, and also in the partial completion of a pilot's universal sighting system. A total of 24 projects was completed during the period 1 February 1942 to 30 September 1945. Of these, 16 were Naval Ordnance projects, 3 were for the Army Air Forces, 2 for the Bureau of Aeronautics, and 3 were exploratory NDRC projects. In addition to the 28 sets of experimental apparatus which were made and tested at service establishments, 8 volumes of technical reports including 125 project reports were completed as a result of the investigations. The research and development work was performed in the main building of The Franklin Institute. Facilities, personnel, laboratory space, purchasing, accounting, and all the necessary services required were provided upon a top priority basis. The Institute was fortunate in having a nucleus of scientific personnel, laboratories, and an excellent machine shop available to accomplish the initial phases of the contract work.

Preliminary contract negotiations were made in January 1942 by Dr. Henry B. Allen, Secretary and Director of the Institute, with Dr. S. H. Caldwell, then Chief of Section D-2, NDRC; plans were discussed with the staff, and on February 1st the original work was started. F. W. Schlesinger, Director of Astronomy and of the Fels Planetarium; I. M. Levitt, Assistant Director of the Planetarium; W. P. West, Assistant Associate Director of Electrical Engineering; and R. H. McClarren, Assistant Associate Director of Aviation and Mechanical Engineering, were transferred from regular Institute duties to the special research and development problems. Shortly thereafter, R. K. Marshall, Assistant Director of the Planetarium, and W. F. Ehringer of the electrical staff joined the research group. In addition to the scientific staff, valuable and necessary service was rendered by all the staff of the Institute: R. W. Lloyd, Vice-President, who acted as top administrator of the contract work; W. F. Jackson, Jr., Business Manager; S. J. Clevenger, Controller; L. G. Schlehner, Building Superintendent; J. H. Jackson, Purchasing Agent; and many others including the Guides, who performed guard duties.

As the number of employees grew and the requirements for laboratory areas increased, more and more space was provided from museum activity. However, this space was so chosen and segregated from the museum activities of the Institute that only those working on the project were aware of the secret nature of the work.

The first project assigned for investigation was the development of a special dive bomb sight, and the members of the newly formed staff looked forward to the early completion of an experimental unit so that they might soon have the feeling they were participating actively in

the war. However, the design of an experimental sight was never started. About the time certain analytical and mathematical analyses of the problem were finished, in late February 1942, NDRC had a more urgent problem. Consequently, all work was stopped on the dive bomb sight, and the full capacity of the laboratory group was devoted to the study, design, and development of a computing-type of stabilized torpedo director.

TORPEDO DIRECTORS.

Within a few weeks the theory and analysis of the problem had been digested and a study model of the director, constructed. Dr. Caldwell

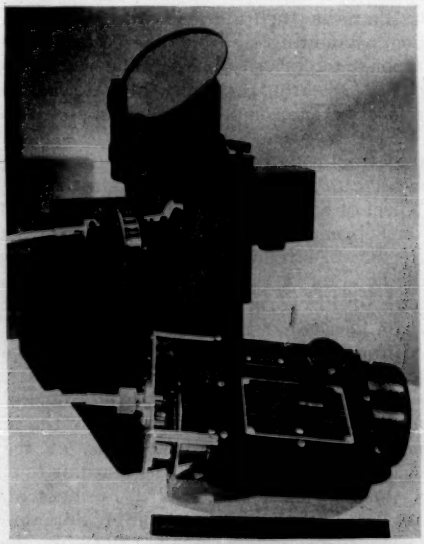

FIG. 1. The Mark 8 torpedo director adapted for automatic inputs and computation of lead angle.

and his Technical Aide, George H. Philbrick, were, in this as well as in all subsequent projects, of great help and assistance. Mr. Harry Jones and R. W. Pitman had been added to the staff. Mr. Pitman, formerly research engineer at the Underwood Elliott Fisher Co., designed the first experimental torpedo director. This marked the beginning of a series of developments of torpedo directors which occupied much of his time and the time of part of the staff throughout the war.

The first experimental torpedo director was tested for principle of operation in a PBY airplane at Naval Air Station, Norfolk, Virginia. Two auxiliary pieces of apparatus were developed for use with this torpedo director. One, an a-c. controller and servomechanism, maintained a stabilized input to the director. The other was a two-phase stabilizer controller with a similar, yet different, servomechanism. During the time of test referred to above, a later development from the experimental model called the Mark 32 torpedo director was also tested at the Naval Air Station, Norfolk—this time in a torpedo bomber aircraft, TBM.

The second director is similiar to 25 such directors built by the International Business Machines Corp. in accordance with Franklin Institute

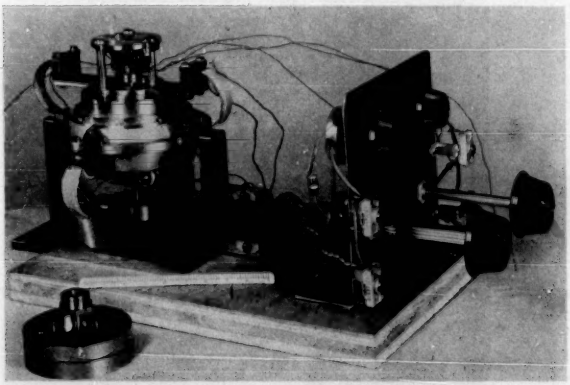

FIG. 2. Experimental gyro used in investigations of lead computing gun sights.

designs and requirements. These directors were used by naval establishments for service tests conducted during the period February 1943 to June 1943. Later production models were installed on torpedo bombers for use in the Pacific theater of operation. Continued investigations produced, in the torpedo director development, many improvements over the first two models. During these investigations special attention was given to developing test equipment for use on motor torpedo boats. Toward the end of the war the latest improvements in radar and other fire control aids were being designed into an advanced type of torpedo director sight, as indicated in Fig. 1.

GUNNERY STUDIES AND SIGHTING SYSTEMS.

Shortly after initiating the investigations on torpedo directors the Institute was asked to perform a series of controlled experiments on the

application of lead computing sights to the flexible guns used in bomber aircraft, to build apparatus suitable for conducting such tests, and to develop certain experimental gun sights. By this time the staff had been augmented by additions including H. A. Van Dyke, Foxboro representative in Philadelphia, Penna.; J. D. Eisler, Stanolind Research Laboratories in Tulsa; E. F. Allen, professor of Physics at Bryn Athyn Academy; Carl Sheppard, technician; U. C. S. Dilks, electrical engineer;

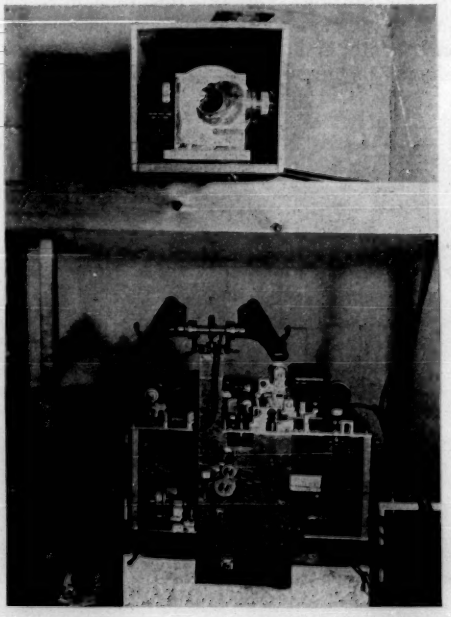

FIG. 3. Mechanical tracking mechanism used to study the behavior of lead computing sights.

and Frank Smith, mechanical designer. Figure 2 shows an experimental gyro constructed for laboratory studies of various methods for indicating gyroscopic precessional force. The advantage of gyroscopic gun sights was appreciated during 1940 by both British and American scientists, and several treatises on the subject were prepared by the Applied Mathematics Panel of NDRC. Fortified with their reports and with early experiments conducted on a British gyro gun sight, the Institute embarked upon a series of investigations and developments

which continued throughout the war. Figure 3 shows a mechanical tracking study mechanism designed by H. A. Van Dyke assisted by Professor J. B. Russell, of Section 7.2, NDRC. The device was built to study, under simulated conditions, the tracking problems involved in the use of a lead computing sight. The computing unit, with handlebar controls, and the interior of the target and reticle presentation unit are shown. Two recorders were used to obtain elevation and azimuth errors for both the sight and the guns.

The early success of the data obtained from a series of controlled experiments performed under the direction of consulting psychologists, Dr. Malcolm Preston, and Dr. Francis Irvin of the University of Penn-

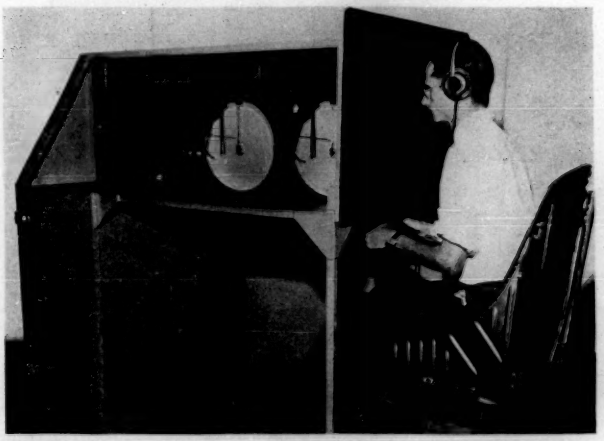

FIG. 4. Electronic tracking study mechanism showing the operators (subject) station and the control-recorder panels.

sylvania, led to immediate changes in the designs and requirements for further production orders of turrets and flexible gun controls. The unquestionable advantage of specially controlled tracking and of the use of lead computing sights was demonstrated, and an additional tracking study mechanism was designed and built. The operator's station and the recording and control panels of this mechanism are shown in Fig. 4, and the electronic computing apparatus is illustrated in Fig. 5. In late 1944 the mechanism was revised to permit studies and the accumulation of data with the subject located in a turret assembly. Figure 6 shows the cathode-ray tube used for target and sight presentation and the other special equipment attached to the turret for the tests.

BOMB SIGHTS.

The development of special bomb sights was another major field of endeavor in which the Institute engaged. W. F. Schlesinger and I. M. Levitt took a leading part in this work. Figure 7 shows VASS Model 1 bomb sight, designed and built in nine days during August 1942 and tested by G. A. Philbrick of NDRC on the tenth day at the Anti-Submarine Development Unit, Atlantic Fleet, Quonset, R. I. So suc-

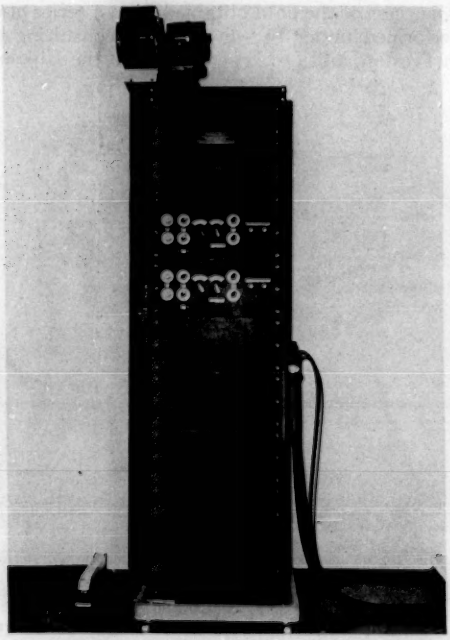

FIG. 5. Amplifiers, power supplies and electronic computer apparatus used with the tracking mechanism.

cessful was the use of this experimental equipment that expansion of the development and another model were requested immediately. Within a period of one month Model 2, illustrated in Fig. 8, was developed and made available for tests. These sighting units were based upon a principle suggested by Commander A. B. Vossler, then Commanding Officer of the Anti-Submarine Development Unit, Atlantic Fleet. To incorporate desired improvements Model 3, shown in Fig. 9, was designed.

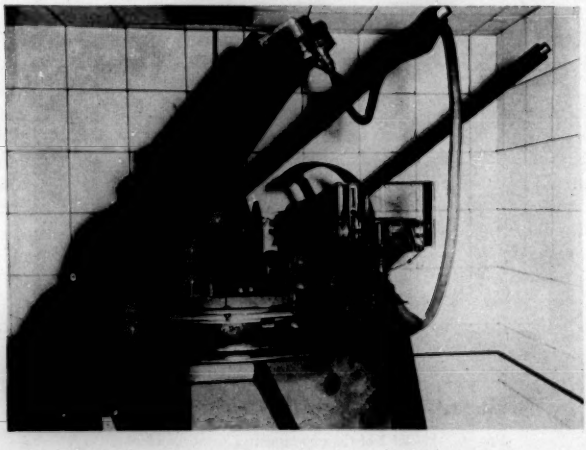

FIG. 6. A Martin upper turret equipped with target and sight presentation apparatus.

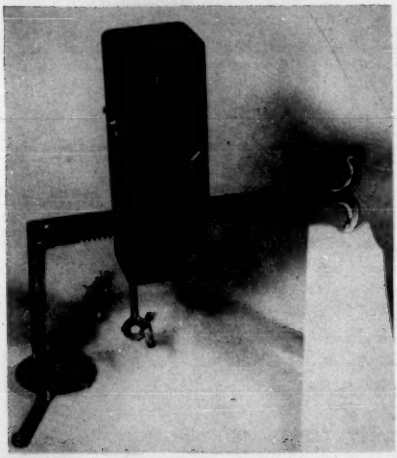

FIG. 7. The first experimental hand-held low-level bomb sight. VASS Model 1.

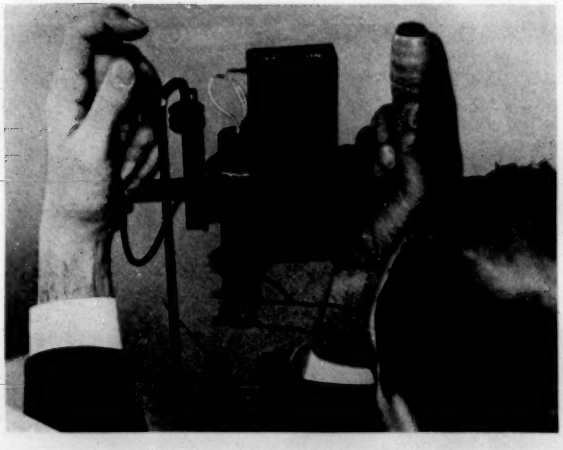

FIG. 8. Model 2 of the experimental VASS bomb sight.

FIG. 9. Prototype production model of the VASS bomb sight.

Three Model 3 units were completed in February 1943 and demonstrated by NDRC to AAF, Wright Field, to the Anti-Submarine Warfare Unit in Boston, and to the Anti-Submarine Command, AAF, in New York. Airborne tests were made at ASDEVLANT, Quonset, R. I.

Model 3, though small, was rather a complicated mechanism, and to meet the requirements of the Navy Department, who desired 60 units for immediate service test and use in the North Atlantic, Model 4 (Fig. 10) was designed by R. W. Pitman. When the designs were completed and a prototype model constructed, no contractor could be found to build the 60 units. Consequently the research and development activity of the Institute was changed temporarily to a production activity.

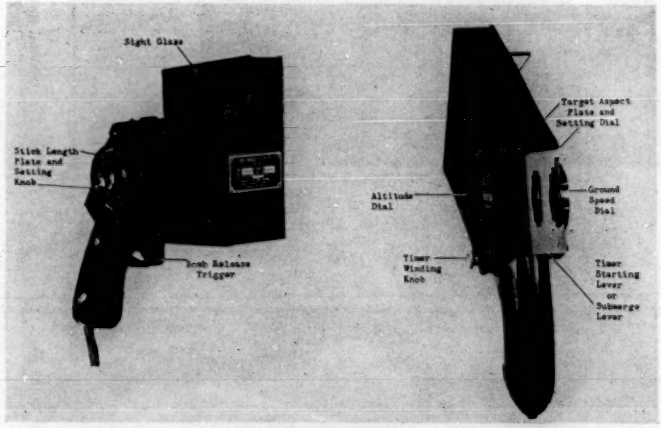

FIG. 10. The Mark 20 hand-held low-level bomb sight.

Some 20 subcontractors were obtained to supply parts, and the units were assembled in the Institute's limited laboratory space. The aid of a considerable number of the secretarial and executive staff of the Institute was enlisted to check the parts, assemble them, and paint the radium dials. Even the wife of the vice-president was conscripted. The 60 sights were produced and delivered to the Navy within three months. Some of these sights, designated as the Mark 20 bomb sight, saw service in the North Atlantic.

Several auxiliary instruments were developed to improve the use and accuracy of the Mark 20 bomb sight. One of these, a direct, electric-drive, potentiometer-type servomechanism, developed by U. C. S. Dilks for use with a radio altimeter, is shown in Fig. 11. Another (Fig.

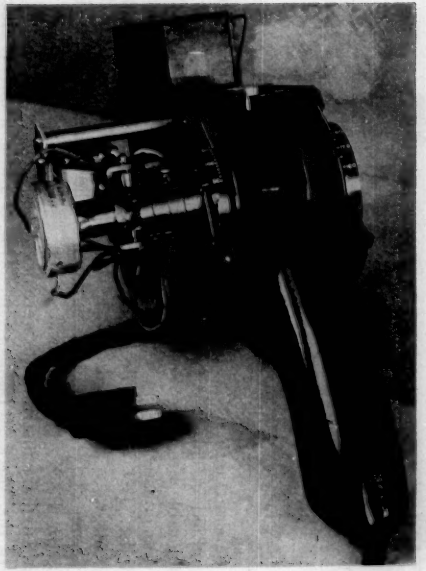

FIG. 11. Altitude servo unit attached to the Mark 20 bomb sight.

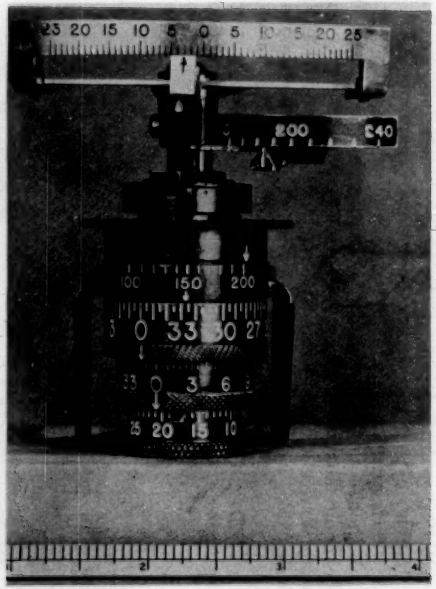

FIG. 12. Ground speed computer for use with the Mark 20 bomb sight.

12) was a small, compact, ground-speed computer for use with the Mark 20 bomb sight. In addition to showing ground speed, this computer would indicate the angle necessary for the pilot to establish a collision course with the target. The conception and development of hand-held bomb sights for use in low-level bombing maneuvers, as illustrated by the Mark 20, established a precedent for further work in the field. Several experimental models of the sights were constructed and tested. The example shown in Fig. 13 employs a rate principle of operation and does not need the vertical reference required by the Mark 20 bomb sight. Strain gages applied to flexure mounts were used as rate indicators connected to a bridge and amplifier unit. In this development a competitive sight, operating, however, on the same principles,

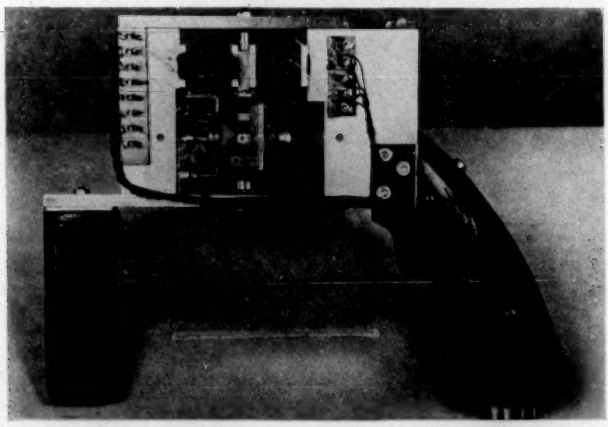

FIG. 13. An experimental rate type of sight developed for use in low altitude bombing.

was placed in production and used during the latter part of the war. The hand-held bomb sight in Fig. 14, designed especially for use on blimps, was tested at the Naval Air Station, Lakehurst, N. J., and at the Naval Air Station, Banana River, Florida. This sight proved very accurate for guiding the release of bombs from blimps. Mr. J. A. Bevan took a leading part in this work.

A slant-range computer (Fig. 15) was produced to allow the bomber a ready means for computing slant range from the aircraft to the target. Values of altitude and ground speed were set by turning the knob to the index line and reading slant range directly off the pointer. Means were provided also for rotating the range scale so the pointer would indicate the horizontal range, should this information be desired.

The inverse of a slant-range computer was developed to permit an observer at a potential target to determine at what position an airplane must release a bomb to hit the target, once the speed and altitude of the bomber had been determined. This item, referred to as an inverse bomb sight, was projected for use on surface vessels.

Figure 16 shows an interesting piece of apparatus designed and built to operate in conjunction with a bombing trainer. This item,

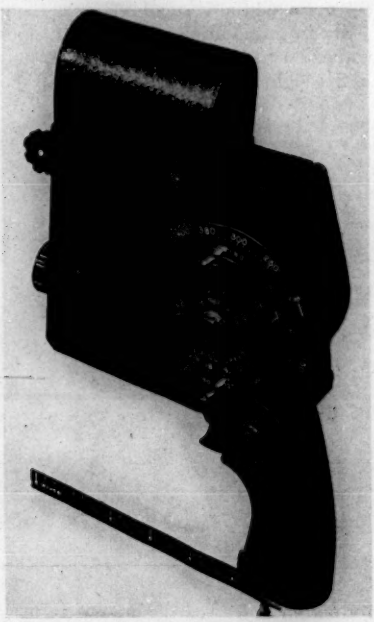

FIG. 14. Special hand-held bomb sight developed for use on blimps.

called a bombing bug, could be remotely controlled to duplicate the motions of maneuvering surface vessels. Several of these units were built to assist the Navy in the training work at the Naval Air Station, Banana River, Fla.

During the latter part of 1943 the Institute was asked to investigate the possibilities of an instrument which would permit pre-set adjustment of the Mark 15 bomb sight. Mr. A. L. Ruiz of Section 7.2 NDRC and Mr. Bevan took a leading part in this activity. Figure 17 illustrates

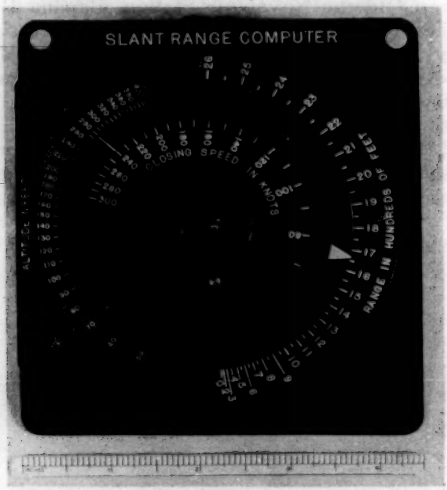

FIG. 15. Slant range computer.

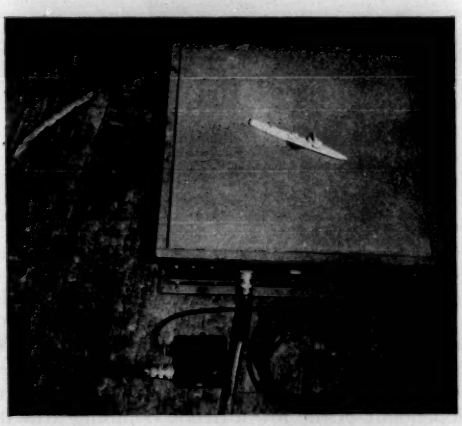

FIG. 16. Bombing bug developed for use with the high altitude bomb sight trainer.

the item delivered to the Naval Air Station, Banana River, Fla., in June 1944. To pre-set the bomb sight the bomber sets in values of air speed, wind speed, target speed, and wind, and stabilized target direction. Closing speed and drift angle are read and normal procedure is used in setting the values in the Mark 15 bomb sight. The unit was built to fit directly upon the stabilizer unit of the bomb sight. Test results showed that the bombing run could be reduced considerably by using the pre-set computer. During the development of this item four models were made. Model 1 consisted of a wood and metal study piece

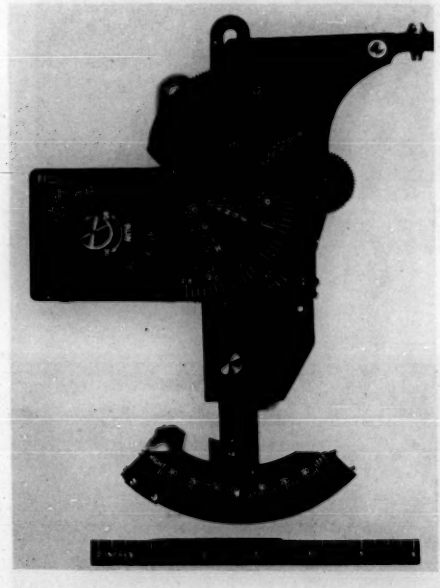

FIG. 17. An experimental pre-set computer for use with the Mark 15 bomb sight.

to check the theoretical investigations and to guide the design group; Model 2 was the first attempt to perfect an operating model; Model 3 was the item tested by both the Army Air Forces and the Navy Bureau of Aeronautics, and Model 4, which completed the work on this project, consisted of a circular slide-rule arrangement for determining the pre-set values independent of the low-altitude bombing attachment to the Mark 15.

In 1944 NDRC assigned the Institute certain projects concerning the development of experimental sights for use with such radio-con-

trolled (guided) missiles as AZON, RAZON, and ROC bombs. The available space facilities in the Institute's building were already overtaxed and the staff, increased to approximately 100 people, was overloaded. Additional experienced research engineers and scientists were not available, and it was necessary to obtain and train individuals for this special type of work. The success of the training program was most encouraging.

After many months of studying and analyzing the problem of sighting and guiding a bomb release from an aircraft to a ground target, a

FIG. 18. Bombing trainer A-5 adopted for Azon and Razon bombing training.

sales engineer-scientist, H. A. Van Dyke, conceived a simple device to perform the job. This device, referred to as CRAB, was used by the Army Air Forces and tested by the Navy Department.

In addition to conceiving, designing, and developing the CRAB sight, the Institute, in cooperation with Columbia University, adapted a Navy A-5 bombing trainer with simulated control equipment and a sighting system for training bombers. Figure 18 illustrates "Miss Guided Missile" in operation. For practice a map of the New York, New Jersey, and Philadelphia area was used, and members of the staff developed a pretty knack for guiding missiles to such targets as the

George Washington Bridge, entrances to the Holland Tunnel, the Pulaski Skyway, Cloverleafs in New Jersey, the Delaware River Bridge, and The Franklin Institute.

ROCKET SIGHTS.

In November 1943 another special group was organized to investigate and develop rocket gunnery sights for airborne use. This work led to the first automatic computing sight for directing the firing of 3½ and 5-in. high-velocity aircraft rockets, the RASP III rocket sight. Except for the manual insertion of target or wind speed and temperature of the

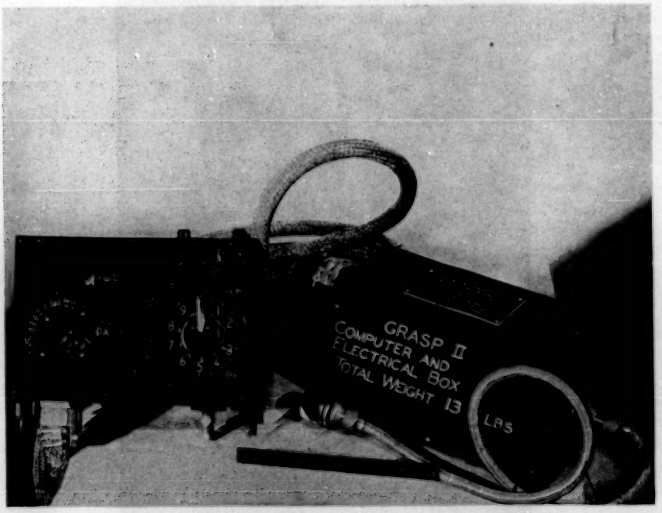

FIG. 19. GRASP Model II, Computer and electric box.

rocket values, the RASP sight is fully automatic. The sight, with its predecessor, Model I, was tested at the Naval Air Station, Quonset, R. I., with U. C. S. Dilks, W. Sheppard and E. C. Lewis in charge of the equipment. More than 700 rockets were fired during the tests of principle and evaluation.

The combination rocket and gun sight shown in Fig. 19 and referred to as GRASP II, was developed by Dr. E. P. Cooper for use with the Mark 23 gun sight to provide a combination sighting system for directing the fire of both guns and forward-firing aircraft rockets. The unit was tested at the Naval Ordnance Testing Station, Inyokern, Calif., during July and August 1945.

PILOT'S UNIVERSAL SIGHTING SYSTEM.

From December 1944 until October 1945 the Institute was commissioned to capitalize upon its work with torpedo directors, bomb sights, gun sight, and rocket sights by investigating and developing a universal sighting system for fighter aircraft. During the war shipborne fighter aircraft, as well as land-based fighters, were performing triple duty; that is, during the invasion of some strategic island group, fighter aircraft would function first as fighters to clear the sky of enemy aircraft, then load with bombs and perform as light bombers, and finally take off with a supply of rockets, dive on enemy gun installations, knock them out, and ease the landing of ground troops. Consequently there was an urgent need for a sighting system which would enable the pilot to direct ammunition in accordance with his particular mission. Work proceeded on the development of the universal sighting system until shortly after V-J day.

The Laboratories of The Franklin Institute, as they exist today, are an outgrowth of the war work. The state of the world at the conclusion of hostilities was such that the Government felt research on all varieties of fire control projects and other military development should be continued in the interests of the national defense. As a consequence, The Franklin Institute established a formal structure for its laboratories in 1946 and placed these laboratories, to an extent, at the disposal of the branches of the armed services. Fire control work continued and numerous other electronic instrument and aircraft problems were undertaken. Moreover it was appreciated that the state of industry in respect to research and development was approximately the same as the state of the Government. Enormous amounts of data had been accumulated in almost all technical fields during the war. For business to operate to the best interests of the public welfare subsequent to the war required an application of the accumulated technical data to improve industrial products and methods. Consequently the Laboratories have acquired a wide variety of facilities for doing research for industrial concerns. A number of contracts have been taken with industrial concerns, and the progress of laboratory work for industry is proceeding quite firmly. We are continuing work for the armed services, in the way that the Institute has always served the country in times of stress. Thus, 124 years after its founding, The Franklin Institute is still broadening its scope of service to the nation and to the public.

Bacteria and Vibrations.—It's doubtful that "looks can kill" but University of Wisconsin scientists know that certain sounds have interesting, often lethal effects—at least on bacteria and protozoa, very small one-celled plants and animals, some of which cause disease.

Sounds or "audible vibrations," to be specific, are being studied by Eugene Ackerman, research assistant to H. B. Wahlin, Professor of Physics, in an attempt to learn whether they can be useful in research on the chemistry and physics of tissue cells and bacteria.

Vibrations, Ackerman says, have one great advantage for biologic extraction purposes; they will break tissue up into its chemical "parts" without the use of heat which often destroys the very substances biochemists want to study.

They may, in addition, be used to break up cells of micro-organisms to release heat-sensitive cellular enzymes, and he hopes that they may even induce changes in heredity in certain forms of life by changing chromosome structure. Yeast and liver extracts can be manufactured without the use of heat.

The vibrations are produced by three devices designed by Ackerman. Two of the vibrators, which differ from one another only in size, are based on the same principle as a telephone receiver, each having a magnetic coil which causes vibration in a thin metal disk. The third vibrator has a plunger which can be lowered into a container of liquid.

When in operation they sound like a radio with a bad tube—but each can kill protozoa in small quantities of liquid within a matter of minutes. Bacteria are affected just as lethally, but it sometimes takes slightly longer.

The smallest vibrator will hold about a teaspoon of bacteria, mold spores, virus, liver, or yeast, in solution, and the larger will hold about a tablespoonful. The third device will induce vibrations in a test-tube full of liquid.

One practical use for the vibrators has been in the field of virus research. Scientists in the college of agriculture believe they may be helpful in learning the nature of two viruses with which they are working.

These viruses cause a disease in chicken embryos, and appear to be a mixture of two different kinds. It is hoped the selective action of the vibrators will destroy one virus to let scientists know which of the two causes disease, or if both play a part. The viruses can be seen only under the electron microscope.

Although vibrations have been used previously in some biologic research, Ackerman will study the effect on tissue and bacteria of vibrations over the whole audible range—from basso profundo to the highest soprano, to use an operatic analogy.

"No one to our knowledge has studied more than one or two frequencies," Ackerman said. "I've been working on the development of magnetic vibrators with an adjustable pitch."

It is possible, scientists say, for particular frequencies to be more efficient in breaking up tissue, just as certain X-rays and ultraviolet light frequencies have advantages others do not.

Work has been done at other laboratories with super-sonic vibrations, which are above the frequencies audible by the human ear, but these have attendant heating capacities which often destroy their usefulness for biologic extraction purposes.

THE EFFECTIVE PATH LENGTH THROUGH A VERTICAL COSMIC-RAY TELESCOPE.*

BY

ENOS E. WITMER [1] AND MARTIN A. POMERANTZ.[2]

I. INTRODUCTION.

One of the most widely used methods for investigating the properties of the cosmic radiation involves measurement of their absorption in matter. By means of coincidence-counter telescopes (see Fig. 1) which record an event only when every member of a train of Geiger-Mueller counters is discharged simultaneously by an ionizing particle, it is possible to select rays which have followed paths lying within specified limits. Thus, a path may be defined such that all of the rays actuating the apparatus must pass through an absorber interposed between successive counter trays. From observations of the counting-rate of the telescope as a function of the thickness and nature of the interposed absorber, the desired information is obtained.

In practice, owing to the finite aperture of the counter train, it is evident that the cosmic-ray particles detected in a particular absorption experiment may traverse total paths varying in length from L, the perpendicular separation between extreme trays, to $(L^2 + l^2 + w^2)^{\frac{1}{2}}$, the diagonal distance between opposite corners. For an accurate analysis of the results, it is thus necessary to determine the average path length through the telescope with respect to all of the radiation concerned, in order to obtain a factor for converting the measured thickness of the interposed material to effective thickness as regards absorption properties. The necessity for applying this correction has only rarely been appreciated (1),[3] and, as the following results indicate, the contribution is not always negligible. The error may become especially serious in the comparison of results obtained with different counter trains.

The effective path length must of course be calculated with respect to a particular dependence upon zenith angle θ of the unidirectional cosmic-ray intensity, $I(\theta)$, defined as the number of ionizing particles per square centimeter per unit solid angle per second arriving in a given direction. It has been established for some time that, at sea level, the variation is in good accord with the equation (2,3,4,5)

$$I(\theta) = I(0) \cos^2 \theta. \tag{1}$$

* The investigations described herewith were supported in part by the Office of Naval Research.

[1] Randal Morgan Laboratory of Physics, University of Pennsylvania, Philadelphia, Penna.

[2] Bartol Research Foundation of The Franklin Institute, Swarthmore, Penna.

[3] The boldface numbers in parentheses refer to the references appended to this paper.

At an altitude of 4300 m. approximately the same law (1) applies to high energy mesons having ranges exceeding 15 cm. of Pb, whereas for the soft component the exponent may be 3. A departure from this relationship apparently occurs at higher altitudes, as was shown by Swann, Locher and Danforth (6), who obtained a value of 0.21 for the ratio $I\ (90°)/I(0°)$.

In order to compare absorption measurements made in the stratosphere with those obtained at low altitudes, it is evidently important to ascertain, for the particular cosmic-ray telescopes utilized in obtaining the data, the magnitude of the dependence of the effective path length upon the nature of the angular distribution of cosmic-ray intensity. For this purpose, calculations have been based upon several different laws in addition to (1), representing alternative possible modes for the variation of intensity with zenith angle. At extremely high altitudes, such as have been attained by apparatus carried aloft in free

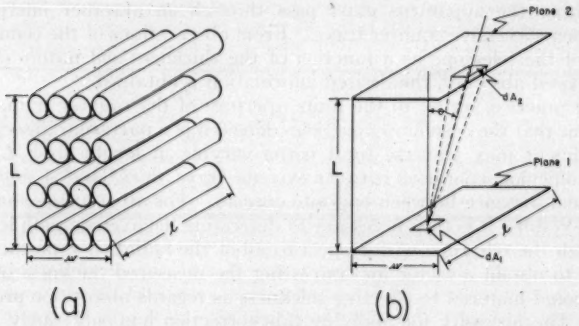

FIG. 1.

balloons during investigations conducted by one of the authors (7), the correct law probably lies within the range considered. Formulas have have been obtained, and families of curves have been computed showing the average path length through a cosmic-ray telescope as a function of all of the dimensions of the apparatus (8). These results may be utilized for obtaining corrections to be applied to the previously reported data of numerous investigators, or for designing systems for experiments at high altitudes in a manner such as to minimize the effects of changes in the directional characteristics of the cosmic radiation.

II. MATHEMATICAL DERIVATIONS.

A. Theory.

The trays in this cosmic-ray telescope are assumed to be rectangular and of length l and width w. The vertical distance between the upper-

most and lowest trays is L. As shown in Fig. 1 the x axis is taken to coincide with one of the long edges of the lowest tray, and the z axis is vertical. The lowest tray is designated plane 1 and the cartesian coordinates of a point in it are $(x_1, y_1, 0)$. The uppermost tray is designated plane 2 and the coordinates of a point in it (x_2, y_2, L).

Consider two elements of area, dA_1 in the lowest tray and dA_2 in the uppermost tray. The cosmic rays which pass through both of these elements of area make an angle θ with the vertical. The number of cosmic rays which pass through both dA_1 and dA_2 per unit time is given by dN, where

$$dN = I(\theta) d\omega \, dA_1 \cos\theta, \tag{2}$$

where $d\omega$ is the solid angle which dA_2 subtends at dA_1. Obviously

$$d\omega = \frac{dA_2 \cos\theta}{\lambda^2}, \tag{3}$$

where λ is the distance from dA_2 to dA_1.

$I(\theta)$ is a constant for any given direction, but will depend upon the zenith angle θ, if the cosmic-ray intensity varies with θ. Substituting Eq. 3 in Eq. 2,

$$dN = \frac{I(\theta) dA_1 dA_2 \cos^2\theta}{\lambda^2}. \tag{4}$$

The most common formula given for the dependence of cosmic-ray intensity on zenith angle is represented by Eq. 1.

We will assume

$$I(\theta) = I(0) \cos^p \theta. \tag{1a}$$

Then

$$dN = \frac{I(0) dA_1 dA_2 \cos^{p+2}\theta}{\lambda^2}. \tag{5}$$

But from Fig. 1

$$\cos\theta = \frac{L}{\lambda}. \tag{6}$$

Hence,

$$dN = \frac{I(0) L^{p+2} dA_1 dA_2}{\lambda^{p+4}}. \tag{7}$$

Also

$$\lambda^2 = L^2 + (y_2 - y_1)^2 + (x_2 - x_1)^2 \tag{8}$$

and

$$\left.\begin{aligned} dA_1 &= dx_1 dy_1 \\ dA_2 &= dx_2 dy_2. \end{aligned}\right\} \tag{9}$$

If $\bar{\lambda}$ is the average path length through the cosmic-ray telescope,

obviously

$$\bar{\lambda} = \frac{\int \lambda dN}{\int dN}. \tag{10}$$

This gives

$$\bar{\lambda} = \frac{\int_0^w dy_1 \int_0^w dy_2 \int_0^l dx_1 \int_0^l \frac{dx_2}{\lambda^{p+3}}}{\int_0^w dy_1 \int_0^w dy_2 \int_0^l dx_1 \int_0^l \frac{dx_2}{\lambda^{p+4}}}. \tag{11}$$

For any value of p the problem consists in evaluating integrals of the type

$$C_n \equiv \int_0^w dy_1 \int_0^w dy_2 \int_0^l dx_1 \int_0^l \frac{dx_2}{\lambda^n}. \tag{12}$$

We consider the cases when

$p = 2, 1, 0,$ and -1, so that
$n = 2, 3, 4, 5,$ and 6.

B. Two-Dimensional Problem ($w \ll 1$).

In the special case when w is so small that variation in y can be neglected

$$\bar{\lambda} = \frac{A_{p+3}}{A_{p+4}}, \tag{13}$$

where

$$A_n \equiv \int_0^l dx_1 \int_0^l \frac{dx_2}{[L^2 + (x_2 - x_1)^2]^{n/2}}. \tag{14}$$

Even when dealing with the general case where the variation in y cannot be neglected, it is worth while evaluating the A_n first, because by merely substituting $\sqrt{L^2 + (y_2 - y_1)^2}$ for L in these results one has the result of carrying out the two integrations in x_1 and x_2 in Eq. 12. Furthermore, the work of evaluating A_n is so easy for all n considered here that it is not necessary to give the details of the process of integration but merely the results as follows:

$$A_2 = \frac{2l}{L} \tan^{-1} \frac{l}{L} - \log \frac{L^2 + l^2}{L^2}, \tag{15}$$

$$A_3 = \frac{2}{L^2} \sqrt{L^2 + l^2} - \frac{2}{L}, \tag{16}$$

$$A_4 = \frac{l}{L^3} \tan^{-1} \frac{l}{L}, \tag{17}$$

$$A_5 = \frac{4}{3L^4}\sqrt{L^2 + l^2} - \frac{2}{3L^3} - \frac{2}{3L^3\sqrt{L^2 + l^2}}, \tag{18}$$

$$A_6 = \frac{1}{4L^4} - \frac{1}{4L^2(L^2 + l^2)} + \frac{3l}{4L^5}\tan^{-1}\frac{l}{L}. \tag{19}$$

It is desirable for both theoretical and practical reasons to write the formulas for $\bar{\lambda}$ in dimensionless form. For this reason we introduce $B_n(u)$, where

$$B_n(u) \equiv L^{n-2}A_n \tag{20}$$

and

$$u \equiv \frac{l}{L}. \tag{21}$$

It follows that

$$B_2(u) = 2u\tan^{-1}u - \log(1 + u^2), \tag{22}$$

$$B_3(u) = 2\sqrt{1 + u^2} - 2, \tag{23}$$

$$B_4(u) = u\tan^{-1}u, \tag{24}$$

$$B_5(u) = \frac{4}{3}\sqrt{1 + u^2} - \frac{2}{3(1 + u^2)} - \frac{2}{3}, \tag{25}$$

$$B_6(u) = \frac{3}{4}u\tan^{-1}u - \frac{1}{4(1 + u^2)} + \frac{1}{4}. \tag{26}$$

Substituting Eq. 20 in Eq. 13,

$$\frac{\bar{\lambda}}{L} = \frac{B_{p+3}(u)}{B_{p+4}(u)}, \tag{27}$$

where, as indicated in Eq. 1a, p determines the dependence of the intensity on zenith angle.

1. Series Approximations when $u < 1$.

$p = 2$ ($\cos^2\theta$ distribution):

$$\frac{\bar{\lambda}}{L} = 1 + \frac{1}{12}u^2 - \frac{1}{15}u^4 + \frac{377}{6720}u^6 - \frac{29}{600}u^8 + \cdots. \tag{28}$$

$p = 1$ ($\cos\theta$ distribution):

$$\frac{\bar{\lambda}}{L} = 1 + \frac{1}{12}u^2 - \frac{41}{720}u^4 + \frac{263}{6048}u^6 - \cdots. \tag{29}$$

$p = 0$ (isotropic distribution):

$$\frac{\bar{\lambda}}{L} = 1 + \frac{1}{12}u^2 - \frac{17}{360}u^4 + \frac{391}{12\,096}u^6 - \frac{44\,089}{1\,814\,400}u^8 + \cdots. \tag{30}$$

$p = -1$ (*sec. θ distribution*):

$$\frac{\bar{\lambda}}{L} = 1 + \frac{1}{12}u^2 - \frac{3}{80}u^4 + \frac{19}{840}u^6 - \cdots. \tag{31}$$

All these series formulas are approximations valid only when $u < 1$.

It is interesting to note that for all the values of p considered:

$$\frac{\bar{\lambda}}{L} = 1 + \frac{1}{12}u^2 + \cdots \tag{32}$$

to that degree of approximation.

A study of the coefficients in formulas 28 to 31 shows that the numerical values obtained with the different distribution laws differ only slightly except when u is large. This is in accordance with the results of a qualitative approach to this problem.

C. Three-Dimensional Problem.

1. Evaluation of C_n.

We will now evaluate the integrals C_n defined in Eq. 12.

$n = 2$:

From Eqs. 12 and 15

$$C_2 = 2l\int_0^w dy_1\int_0^w \frac{1}{\sqrt{L^2+(y_2-y_1)^2}}\tan^{-1}\frac{l}{\sqrt{L^2+(y_2-y_1)^2}}\,dy_2 - \int_0^w dy_1\int_0^w \log\left[L^2+l^2+(y_2-y_1)^2\right]dy_2 + \int_0^w dy_1\int_0^w \log\left[L^2+(y_2-y_1)^2\right]dy_2. \tag{33}$$

The only one of the three integrals on the right that offers any difficulty is the first. It is evaluated by making the substitution:

$$\tan^{-1}\frac{l}{\sqrt{L^2+(y_2-y_1)^2}} = \sin^{-1}\frac{l}{\sqrt{L^2+l^2+(y_2-y_1)^2}}. \tag{34}$$

Then

$$\int_0^w dy_1\int_0^w \frac{1}{\sqrt{L^2+(y_2-y_1)^2}}\tan^{-1}\frac{l}{\sqrt{L^2+(y_2-y_1)^2}}\,dy_2 = \int_0^w dy_1\int_0^w \frac{1}{\sqrt{L^2+l^2+(y_2-y_1)^2}} \times\left[1-\frac{l^2}{L^2+l^2+(y_2-y_1)^2}\right]^{-\frac{1}{2}}\sin^{-1}\frac{l}{\sqrt{L^2+l^2+(y_2-y_1)^2}}\,dy_2 = \sum_{r=0}^{\infty}\left\{\sum_{j=0}^{r}\frac{(2r-2j)!}{[(r-j)!]^2}\cdot\frac{(2j)!}{(j!)^2}\cdot\frac{1}{(2j+1)}\right\}\frac{l^{2r+1}}{2^{2r}}G_r', \tag{35}$$

where

$$G_r' \equiv \int_0^w dy_1 \int_0^w \frac{dy_2}{[L^2 + l^2 + (y_2 - y_1)^2]^{r+1}}. \tag{36}$$

This result is obtained by expanding the $\sin^{-1}$ and the square bracket in the integrand. The integration (9) of Eq. 36 yields:

$$G_0' = \frac{2w}{\sqrt{L^2 + l^2}} \tan^{-1} \frac{w}{\sqrt{L^2 + l^2}} - \log \frac{L^2 + l^2 + w^2}{L^2 + l^2}, \tag{37}$$

$$G_1' = \frac{w}{(L^2 + l^2)^{\frac{1}{2}}} \tan^{-1} \frac{w}{\sqrt{L^2 + l^2}} \tag{37a}$$

and for $r \geqslant 2$

$$G_r' \equiv \frac{1}{(L^2 + l^2)^r} \sum_{\sigma=1}^{r-1} \frac{(2r)!}{(2r - 2\sigma + 1)!} \frac{[(r - \sigma)!]^2}{2^{2\sigma}(r!)^2} \cdot \frac{1}{(r - \sigma)}$$

$$- \sum_{\sigma=1}^{r-1} \frac{(2r)!}{(2r - 2\sigma + 1)!} \frac{[(r - \sigma)!]^2}{2^{2\sigma}(r!)^2} \cdot \frac{1}{(r - \sigma)} \frac{1}{(L^2 + l^2)^\sigma}$$

$$\times \frac{1}{(L^2 + l^2 + w^2)^{r-\sigma}} + \frac{2(2r)!}{2^{2r}(r!)^2} \cdot \frac{w}{(L^2 + l^2)^{r+\frac{1}{2}}} \tan^{-1} \frac{w}{\sqrt{L^2 + l^2}}. \tag{37b}$$

Then

$$C_2 = (L^2 + l^2 - w^2) \log (L^2 + l^2 + w^2) - (L^2 - w^2) \log (L^2 + w^2)$$

$$- (L^2 + l^2) \log (L^2 + l^2) + L^2 \log L^2 + 4wL \tan^{-1} \frac{w}{L}$$

$$- 4w\sqrt{L^2 + l^2} \tan^{-1} \frac{w}{\sqrt{L^2 + l^2}}$$

$$+ \sum_{r=0}^{\infty} \left\{ \sum_{j=0}^{r} \frac{(2r - 2j)!}{[(r - j)!]^2} \cdot \frac{(2j)!}{(j!)^2} \cdot \frac{1}{(2y + 1)} \right\} \frac{l^{2r+2}}{2^{2r-1}} G_r'. \tag{38}$$

n = 3:

From Eqs. 12 and 16:

$$C_3 = 2 \int_0^w dy_1 \int_0^w \frac{[L^2 + l^2 + (y_2 - y_1)^2]^{\frac{1}{2}}}{[L^2 + (y_2 - y_1)^2]} dy_2$$

$$- 2 \int_0^w dy_1 \int_0^w \frac{1}{[L^2 + (y_2 - y_1)^2]} dy_2. \tag{39}$$

The first integral is evaluated by expanding the numerator of the integrand by the binomial theorem taking $(L^2 + l^2)$ as the larger term.

This gives

$$2\int_0^w dy_1 \int_0^w \frac{[L^2 + l^2 + (y_2 - y_1)^2]^{\frac{1}{2}}}{[L^2 + (y_2 - y_1)^2]}\, dy_2$$

$$= 2\sqrt{L^2 + l^2}\int_0^w dy_1 \int_0^w \frac{dy_2}{[L^2 + (y_2 - y_1)^2]}$$

$$+ 4\sqrt{L^2 + l^2}\sum_{r=1}^{\infty} \frac{(-1)^{r+1}}{2^{2r-1}} \cdot \frac{(2r - 2)!}{(r - 1)!\, r!} \cdot \frac{H_r'}{(L^2 + l^2)^r}. \quad (40)$$

Here

$$2H_r' \equiv \int_0^w dy_1 \int_0^w \frac{(y_2 - y_1)^{2r} dy_2}{[L^2 + (y_2 - y_1)^2]}. \quad (41)$$

This integral can easily be evaluated by dividing the denominator into the numerator; there is a remainder term. This gives

$$H_r' = \sum_{\sigma=0}^{r-1} \frac{(-1)^\sigma L^{2\sigma} w^{2r-2\sigma}}{(2r - 2\sigma)(2r - 2\sigma - 1)}$$

$$+ (-1)^r L^{2r-1} w \tan^{-1}\frac{w}{L} - (-1)^r \tfrac{1}{2} L^{2r} \log \frac{L^2 + w^2}{L^2}. \quad (42)$$

The final result for C_3 is

$$C_3 = 4\sqrt{L^2 + w^2} - 4L - 2w \log \frac{\sqrt{L^2 + w^2} + w}{\sqrt{L^2 + w^2} - w}$$

$$- 2\sqrt{L^2 + l^2} \log \frac{L^2 + w^2}{L^2} + \frac{4w\sqrt{L^2 + l^2}}{L} \tan^{-1}\frac{w}{L}$$

$$+ 4\sqrt{L^2 + l^2}\sum_{r=1}^{\infty} \frac{(-1)^{r+1}}{2^{2r-1}} \cdot \frac{(2r - 2)!}{(r - 1)!\, r!} \cdot \frac{H_r'}{(L^2 + l^2)^r}. \quad (43)$$

n = 4:

Combining Eq. 12 and 17

$$C_4 \equiv l\int_0^w dy_1 \int_0^w \frac{1}{[L^2 + (y_2 - y_1)^2]^{\frac{1}{2}}} \tan^{-1}\frac{l}{[L^2 + (y_2 - y_1)^2]}\, dy_2. \quad (44)$$

In all the integrations for C_n the independent variable for the first integration should be $(y_2 - y_1)$, with y_1 constant, of course. In this case it is advantageous to use partial integration first in such a way as to get rid of the $\tan^{-1}$ factor by differentiation in the double integral. The first integration in the resulting double integral can be done by separating into partial fractions. *All* the integrands for the integration with respect to y_1 involve a $\tan^{-1}$ term. Once more partial integration can be used in each integral to eliminate the $\tan^{-1}$ term in the resulting integral.

In this way one obtains

$$C_4 = \frac{2l\sqrt{L^2+w^2}}{L^2}\tan^{-1}\frac{l}{\sqrt{L^2+w^2}} + \frac{2w\sqrt{L^2+l^2}}{L^2}\tan^{-1}\frac{w}{\sqrt{L^2+l^2}} - \frac{2l}{L}\tan^{-1}\frac{l}{L} - \frac{2w}{L}\tan^{-1}\frac{w}{L} - \log\frac{L^2(L^2+l^2+w^2)}{(L^2+l^2)(L^2+w^2)}. \quad (45)$$

n = 5:

Using Eqs. 12 and 18

$$C_5 = \frac{4}{3}\int_0^w dy_1\int_0^w \frac{[L^2+l^2+(y_2-y_1)^2]^{\frac{1}{2}}}{[L^2+(y_2-y_1)^2]}dy_2 - \frac{2}{3}\int_0^w dy_1\int_0^w \frac{dy_2}{[L^2+(y_2-y_1)^2][L^2+l^2+(y_2-y_1)^2]^{\frac{1}{2}}} - \frac{2}{3}\int_0^w dy_1\int_0^w \frac{dy_2}{[L^2+(y_2-y_1)^2]^{\frac{1}{2}}}. \quad (46)$$

In the case of the first two integrals the factors in the integrands with the exponent $\frac{1}{2}$ are expanded by means of the binomial theorem in such a way that the positive powers of $(y_2 - y_1)$ appear in all terms except the first. It is exactly the same procedure as that used in evaluating C_3. Therefore the details will not be given. The result is

$$C_5 = \frac{4}{3L} - \frac{4\sqrt{L^2+w^2}}{3L^2} + \frac{4w\sqrt{L^2+l^2}}{3L^3}\tan^{-1}\frac{w}{L} + \frac{2}{3}\sum_{r=1}^{\infty}\frac{(-1)^r}{2^{2r-2}}\cdot\frac{(2r-2)!}{(r-1)!r!}(L^2+l^2)^{-r+\frac{1}{2}}J_r'. \quad (47)$$

Here

$$J_r' = \sum_{\sigma=1}^{r-1}(-1)^{\sigma-1}\frac{w^{2r-2\sigma}L^{2\sigma-2}}{(2r-2\sigma-1)} + (-1)^{r-1}L^{2r-3}w\tan^{-1}\frac{w}{L}. \quad (48)$$

n = 6:

From Eqs. 12 and 19

$$C_6 = \frac{1}{4}\int_0^w dy_1\int_0^w \frac{dy_2}{[L^2+(y_2-y_1)^2]^2} - \frac{1}{4}\int_0^w dy_1\int_0^w \frac{dy_2}{[L^2+l^2+(y_2-y_1)^2][L^2+(y_2-y_1)^2]} + \frac{3l}{4}\int_0^w dy_1\int_0^w \frac{1}{[L^2+(y_2-y_1)^2]^{5/2}}\tan^{-1}\frac{l}{\sqrt{L^2+(y_2-y_1)^2}}dy_2. \quad (49)$$

The second and third integrals are evaluated by the same methods as in the case of C_4, namely by partial integration on integrands involving $\tan^{-1}$ so as to get rid of $\tan^{-1}$ in the resulting *integral* term, and

separation in partial fractions whenever integrands such as those in the second integral appear.

The result is

$$C_6 = \frac{(2l^2 + L^2)w}{2L^4\sqrt{L^2 + l^2}} \tan^{-1} \frac{w}{\sqrt{L^2 + l^2}} + \frac{(2w^2 + L^2)l}{2L^4\sqrt{L^2 + w^2}} \tan^{-1} \frac{l}{\sqrt{L^2 + w^2}} - \frac{w}{2L^3} \tan^{-1} \frac{w}{L} - \frac{l}{2L^3} \tan^{-1} \frac{l}{L}. \quad (50)$$

The infinite series in C_2 and C_3 are convergent for all values of the parameters L, l, and w; and the infinite series in C_5 is convergent provided $w \leqslant l$, a condition which can be satisfied in all cases.

2. Reduction to Dimensionless Form.

Equation 11 may be rewritten as

$$\bar{\lambda} = \frac{C_{p+3}}{C_{p+4}}. \quad (51)$$

For both theoretical and practical reasons it is desirable to write this equation in dimensionless form.

Let

$$D_n(u, v) = L^{n-4}C_n, \quad (52)$$

$$u \equiv \frac{l}{L}, \quad (21)$$

$$v \equiv \frac{w}{L}. \quad (53)$$

Then D_n is dimensionless.

From Eqs. 51 and 52

$$\frac{\bar{\lambda}}{L} = \frac{D_{p+3}(u, v)}{D_{p+4}(u, v)}. \quad (54)$$

This dimensionless equation gives $\bar{\lambda}/L$ for the cosmic-ray distribution determined by the value of p.

Below, the formulas for $D_n(u, v)$ are given:

$n = 2$:

$$D_2(u, v) = \log \frac{1 + u^2 + v^2}{(1 + u^2)(1 + v^2)} + u^2 \log \frac{1 + u^2 + v^2}{1 + u^2} + v^2 \log \frac{1 + v^2}{1 + u^2 + v^2} + 4v \tan^{-1} v - 4v\sqrt{1 + u^2} \tan^{-1} \frac{v}{\sqrt{1 + u^2}} + \sum_{r=0}^{\infty} g_r G_r u^{2r+2}, \quad (55)$$

where

$$g_r = \frac{1}{2^{2r-1}} \sum_{j=0}^{r} \frac{(2r-2j)!}{[(r-j)!]^2} \frac{(2j)!}{[j!]^2} \cdot \frac{1}{(2j+1)}. \tag{56}$$

and

$$G_0 = \frac{2v}{\sqrt{1+u^2}} \tan^{-1} \frac{v}{\sqrt{1+u^2}} - \log \frac{1+u^2+v^2}{1+u^2}, \tag{57}$$

$$G_1 = \frac{v}{(1+u^2)^{\frac{1}{2}}} \tan^{-1} \frac{v}{\sqrt{1+u^2}}, \tag{57a}$$

and for $r \geqslant 2$

$$G_r = \frac{1}{(1+u^2)^r} \sum_{\sigma=1}^{r-1} \frac{(2r)![(r-\sigma)!]^2}{2^{2\sigma}(r!)^2(2r-2\sigma+1)!} \cdot \frac{1}{(r-\sigma)}$$
$$- \sum_{\sigma=1}^{r-1} \frac{(2r)![(r-\sigma)!]^2}{2^{2\sigma}(r!)^2(2r-2\sigma+1)!} \cdot \frac{1}{(r-\sigma)} \cdot \frac{1}{(1+u^2)^\sigma (1+u^2+v^2)^{r-\sigma}}$$
$$+ \frac{(2r)!}{2^{2r}(r!)^2} \cdot \frac{v}{(1+u^2)^{r+\frac{1}{2}}} \tan^{-1} \frac{v}{\sqrt{1+u^2}}. \tag{57b}$$

n = 3:

$$D_3(u,v) = 4\sqrt{1+v^2} - 4 - 2v \log \frac{\sqrt{1+v^2}+v}{\sqrt{1+v^2}-v}$$
$$- 2\sqrt{1+u^2} \log (1+v^2) + 4v\sqrt{1+u^2} \tan^{-1} v$$
$$- 8\sqrt{1+u^2} \sum_{r=1}^{\infty} \frac{(-1)^r (2r-2)!}{2^{2r}(r-1)!r!} (1+u^2)^{-r} H_r, \tag{58}$$

where

$$H_r = \sum_{\sigma=0}^{r-1} \frac{(-1)^\sigma v^{2r-2\sigma}}{(2r-2\sigma)(2r-2\sigma-1)}$$
$$+ (-1)^r v \tan^{-1} v - (-1)^r \tfrac{1}{2} \log (1+v^2). \tag{59}$$

n = 4:

$$D_4(u,v) = 2u\sqrt{1+v^2} \tan^{-1} \frac{u}{\sqrt{1+v^2}}$$
$$+ 2v\sqrt{1+u^2} \tan^{-1} \frac{v}{\sqrt{1+u^2}} - 2u \tan^{-1} u$$
$$- 2v \tan^{-1} v - \log \frac{1+u^2+v^2}{(1+u^2)(1+v^2)}. \tag{60}$$

$n = 5$:

$$D_5(u, v) = \frac{4}{3} - \frac{4}{3}\sqrt{1+v^2} + \frac{4}{3}v\sqrt{1+u^2}\tan^{-1} v + \frac{8}{3}\sum_{r=1}^{\infty}\frac{(-1)^r(2r-2)!}{2^{2r}(r-1)!\,r!}(1+u^2)^{-r+\frac{1}{2}}J_r, \quad (61)$$

where

$$J_r = \sum_{\sigma=1}^{r-1}(-1)^{\sigma-1}\frac{v^{2r-2\sigma}}{2r-2\sigma-1} + (-1)^{r-1}v\tan^{-1} v. \quad (62)$$

$n = 6$:

$$D_6(u, v) = \frac{(2u^2+1)v}{2\sqrt{1+u^2}}\tan^{-1}\frac{v}{\sqrt{1+u^2}} + \frac{(2v^2+1)u}{2\sqrt{1+v^2}}\tan^{-1}\frac{u}{\sqrt{1+v^2}} - \tfrac{1}{2}v\tan^{-1} v - \tfrac{1}{2}u\tan^{-1} u. \quad (63)$$

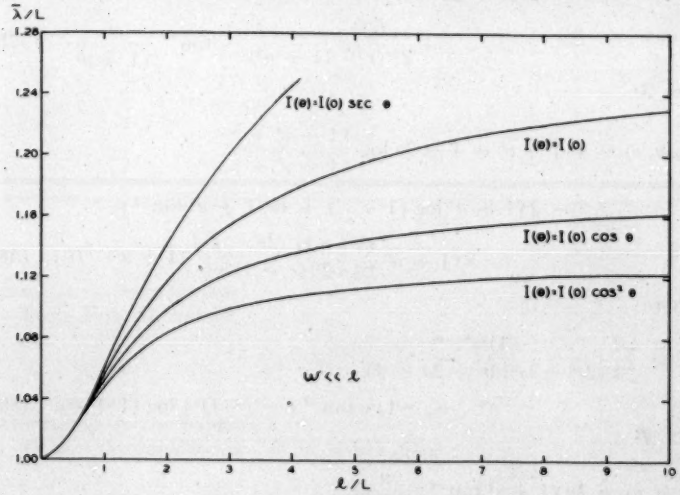

FIG. 2.

III. RESULTS.

The results obtained from numerical computations utilizing the formulas developed in Section II are best presented in a series of graphs.

Figure 2 shows $\bar{\lambda}/L$ (the ratio of the average path length to the normal path length) plotted as a function of l/L (the ratio of counter

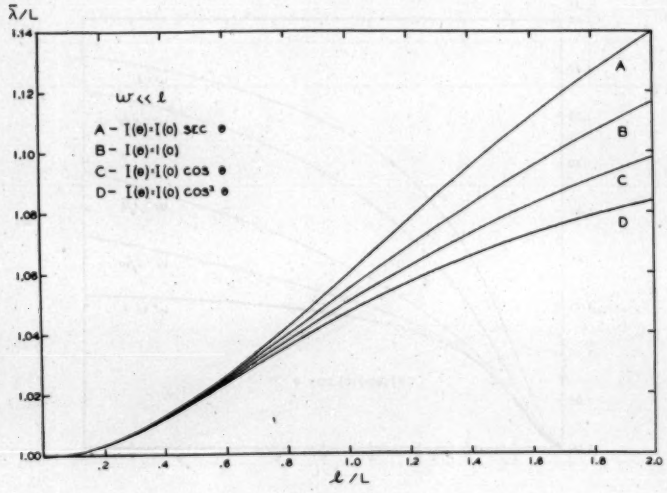
λ̄/L
1.14
1.12
1.10
1.08
1.06
1.04
1.02
1.00
w << l
A – I(θ)=I(0) sec θ
B – I(θ)=I(0)
C – I(θ)=I(0) cos θ
D – I(θ)=I(0) cos² θ
A
B
C
D
.2
.4
.6
.8
1.0
1.2
1.4
1.6
1.8
2.0
l/L

FIG. 3.

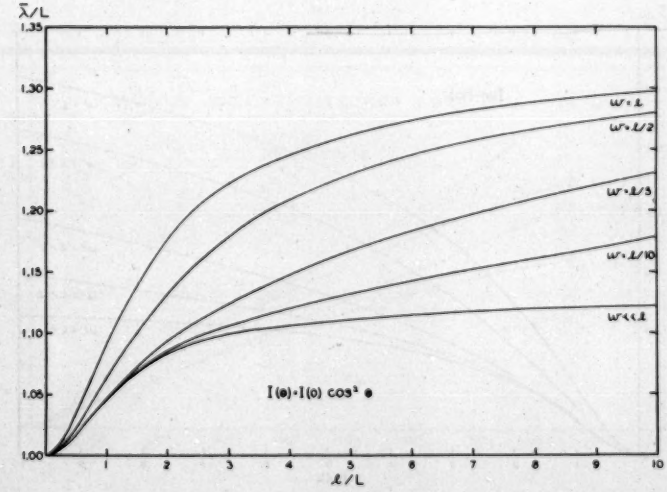
λ̄/L
1.35
1.30
1.25
1.20
1.15
1.10
1.05
1.00
w = l
w = l/2
w = l/3
w = l/10
w << l
I(θ)=I(0) cos² θ
1
2
3
4
5
6
7
8
9
10
l/L

FIG. 4.

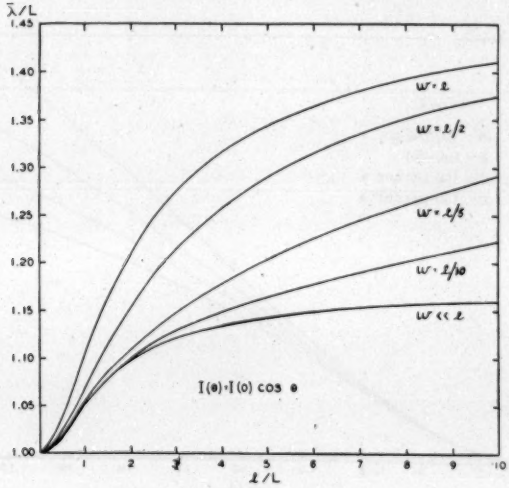
λ̄/L
1.45
1.40
1.35
1.30
1.25
1.20
1.15
1.10
1.05
1.00
1
2
3
4
5
6
7
8
9
10
ℓ/L
W = ℓ
W = ℓ/2
W = ℓ/5
W = ℓ/10
W << ℓ
I(θ) = I(0) cos θ

FIG. 5.

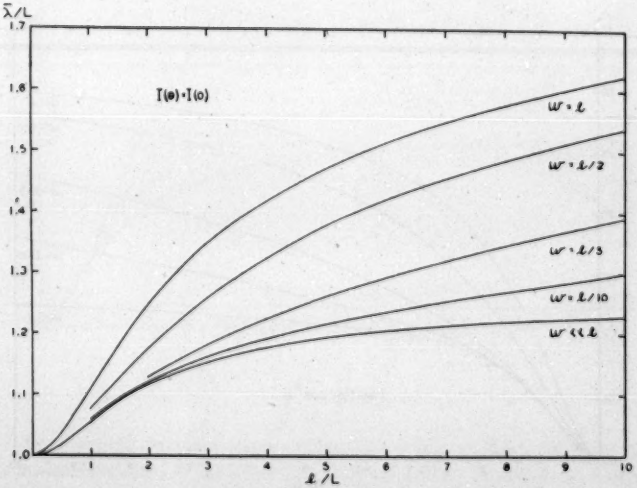
λ̄/L
1.7
1.6
1.5
1.4
1.3
1.2
1.1
1.0
1
2
3
4
5
6
7
8
9
10
ℓ/L
I(θ) = I(0)
W = ℓ
W = ℓ/2
W = ℓ/3
W = ℓ/10
W << ℓ

FIG. 6.

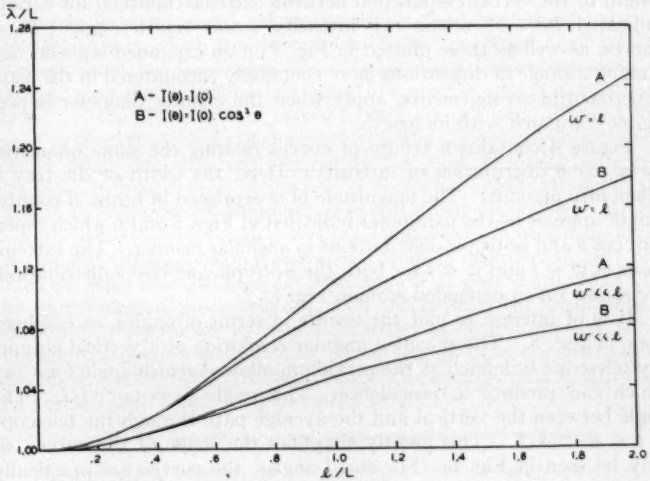
$\bar{\lambda}/L$
1.28
1.24
1.20
1.16
1.12
1.08
1.04
1.00
A - I(θ)=I(0)
B - I(θ)=I(0) cos² θ
A
ω = ℓ
B
ω = ℓ
A
ω << ℓ
B
ω << ℓ
.2
.4
.6
.8
1.0
1.2
1.4
1.6
1.8
2.0
ℓ/L

FIG. 7.

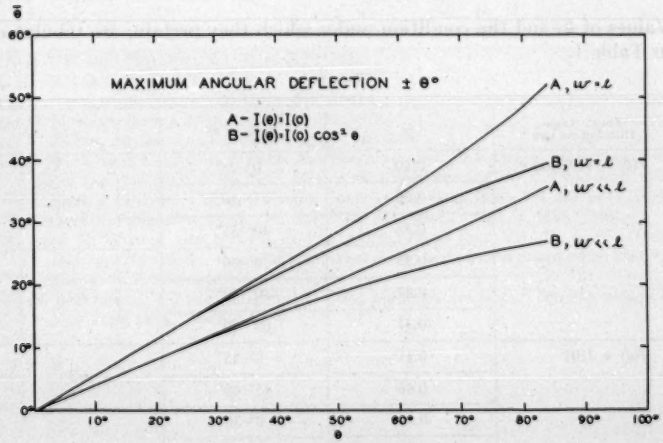
$\bar{\theta}$
60°
50°
40°
30°
20°
10°
0°
MAXIMUM ANGULAR DEFLECTION ± θ°
A - I(θ)=I(0)
B - I(θ)=I(0) cos² θ
A, ω = ℓ
B, ω = ℓ
A, ω << ℓ
B, ω << ℓ
10°
20°
30°
40°
50°
60°
70°
80°
90°
100°
θ

FIG. 8.

length to the vertical separation between extreme counters) for various indicated laws of cosmic-ray intensity *versus* zenith angle. These curves, as well as those plotted in Fig. 3 on an expanded scale encompassing a range of dimensions more commonly encountered in the usual experimental arrangements, apply when the counter diameter is negligible compared with its length.

Figure 4 contains a family of curves relating the same quantities for a $\cos^2\theta$ distribution of intensity. Here, the width of the tray is taken into account. The magnitude of w expressed in terms of counter length appears as the parameter indicated in Figs. 5 and 6 which represent $\cos\theta$ and isotropic distributions in a similar manner. The extreme cases of $w = l$ and $w \ll l$ for both the isotropic and $\cos^2\theta$ distributions are shown on an expanded scale in Fig. 7.

It is of interest to plot the results in terms of angles, as has been done in Fig. 8. The so-called angular resolution of a vertical cosmic-ray telescope is defined as the maximum allowed zenith angle for a ray which can produce a coincidence. This angle $\theta_R = \tan^{-1} l/L$. The angle between the vertical and the average path through the telescope is $\bar{\theta} = \sec^{-1} \bar{\lambda}/L$. This greatly simplifies the shape of the curves, as may be seen in Fig. 8. For small angles, the curves are practically straight lines. Thus, the results are conveniently summarized by the following simple expression

$$\bar{\theta} = k_1 \theta_R. \tag{64}$$

Values of k_1 and the condition under which they pertain, are tabulated in Table I.

TABLE I.

Zenith Angle Distribution Law	k_1	Range of θ_R	w
$I(\theta) = I(0)\cos^3\theta$	0.40	0°–25°	
	0.36	25°–40°	$\ll l$
	0.33	40°–55°	
	0.55	0°–30°	
	0.47	30°–60°	$= l$
	0.37	60°–80°	
$I(\theta) = I(0)$	0.41	0°–45°	$\ll l$
	0.43	45°–80°	
	0.55	0°–30°	
	0.60	30°–60°	$= l$
	0.68	60°–80°	

IV. CONCLUSIONS.

These derivations and calculations have been performed only for arrangements in which the dimensions of the uppermost tray are the same as those for the lowest tray. Other cases concerning trays of different sizes could of course be treated in a manner similar to that used above. If the dimensions of extreme trays are not very different, the use of arithmetical means of the corresponding dimensions should yield results which are sufficiently accurate for most practical purposes. The most striking aspects of the results presented quantitatively in the various figures may be summarized qualitatively as follows: (1) the average path length through a vertical coincidence counter train is not greatly affected by a change in the zenith angle distribution law, provided the separation between extreme trays is roughly comparable with the dimensions of the trays; (2) even for geometrical arrangements which intuitively appear to be unsatisfactory as regards angular definition and the possible complicating effects arising from the distribution of allowed path lengths, the departure of the average path length from the vertical path length may be rather small.

V. ACKNOWLEDGMENTS.

The numerical computations have been performed by Stephen H. Forbes, with the assistance of Henrietta Fricke. It is a genuine pleasure to acknowledge their active participation in this investigation and the invaluable assistance which they have rendered thereby.

REFERENCES.

(1) K. GREISEN, *Phys. Rev.*, Vol. 61, p. 212 (1942).
(2) T. H. JOHNSON, *Phys. Rev.*, Vol. 43, p. 307 (1933).
(3) G. BERNARDINI, *Nature*, Vol. 129, p. 578 (1932).
(4) G. MEDICUS, *Zeits. f. Phys.*, Vol. 74, p. 350 (1932).
(5) L. TUWIM, *Berliner Berichte*, Vol. 19, pp. 91, 360 (1931).
(6) W. F. G. SWANN AND G. L. LOCHER, *Nat. Geog. Soc. Cont. Tech. Papers Stratosphere Series No. 1*, p. 714 (1935). W. F. G. SWANN, G. L. LOCHER and W. E. DANFORTH, *ibid.*, No. 2, p. 13 (1936). W. F. G. SWANN, JOURNAL FRANKLIN INST., Vol. 222, p. 45 (1936).
(7) MARTIN A. POMERANTZ, *Phys. Rev.*, Vol. 73, p. 651 (1948). *Ibid.*, p. 1253 (1948).
(8) ENOS E. WITMER AND MARTIN A. POMERANTZ, *Phys. Rev.*, Vol. 73, p. 651 (1948). *Ibid.*, p. 1274 (1948). A preliminary report of the results herein described in detail has been given in abstract form.
(9) H. B. DWIGHT, "Tables of Integrals and Other Mathematical Data," The Macmillan Co., New York, 1934. See Eq. 120.9.

Eye-Dropper Technique Proves Effective Method of Testing Steel.—Science has removed the eye-dropper from the family medicine cabinet and put it to work sampling molten steel at 2700° F.

The "eye-dropper," as now used industrially in the G. E. Schenectady Works Laboratory, is a heat-resistant glass tube, about the diameter of a lead pencil and 18 in. long, with a rubber bulb at one end. Liquid steel fresh from the furnace is drawn up into the tube by squeezing the rubber bulb, just as an eye-dropper draws up medicine. The steel hardens into a smooth, homogeneous rod within 5 min., the glass is cracked from it, and the rod is ready to be checked for quality.

Eye-dropper samples may be prepared for analysis in a few minutes. Older techniques required long hours and involved such laborious operations as cutting a block from a hardened steel mass, machining it into a rod, and buffing it to a high polish.

Three men, wearing gloves and goggles, form a highly co-ordinated testing team. In a sequence that must take no more than 60 seconds, the first man removes a puddle from the heart of the furnace with a ladle on the end of a 10-ft. pole. A second worker skims away the slag forming on the surface as the metal approaches the solidifying point. The third man then steps forward with the "eye-dropper" to suck up a glowing sample.

Cut in two and fitted into sockets before a spectrograph, the sample forms two electrodes of a high-voltage arc. An electric spark jumps between the two, giving off a light which varies with the makeup of the electrodes. By breaking up this light into its component colors with a prism, trained observers are able to judge the quality of any given batch of steel sampled by the "eye-dropper."

R. H. O.

Results of Conservation.—Conservation endeavors in the United States have already meant much to the Nation and to the world. When World War II boiled up in Europe and the plea for American food was raised again, the farmers of the United States did a far better job of production than in World War I—and they did it with far less devastation of the soil. Just one comparison illustrates the difference. During and immediately after World War I, more than 30 million acres of grass and pasture were plowed up. In World War II, less than 3 million acres unsuited for cultivation felt the plow.

What's New in Plastics (*Plastics*, Vol. 8, No. 7).—A radio active isotope, byproduct of the nation's atomic energy plants, is the heart of a new gage for measuring the thickness of Pliofilm and other thin films on continuous production equipment. Developed by W. E. Morris, of the research laboratory, the Goodyear Tire and Rubber Co., the device is capable of measuring material as thin as one-thousandth of an inch.

A combination edging and folding machine is now available through the Taber Instrument Corporation, North Tonawanda, New York. It will simultaneously bead or fold one or both parallel edges of sheet plastic in like or different beads or folds. The machine can bead or fold 500 to 1000 in. of sheet plastic per minute ranging in gage from 0.005 to 0.020 in. in thickness and from 2 to 20 in. in width.

ELECTRON LENSES OF HYPERBOLIC FIELD STRUCTURE.*

BY

REINHOLD RÜDENBERG.[1]

Part I.

SUMMARY.

From the conditions of focus formation and Laplace's equation, a hyperbolic field structure is derived which permits a rigorous mathematical description and an explicit determination of electron trajectories of any amplitude. Various possible electron paths are formulated and charts are given for the most outstanding solutions, namely for symmetrical electron lenses and mirrors.

The focal properties of such field formations are derived and the results condensed to closed formulations and plots easy to survey. Uniform rays of parallel incidence do not suffer any aberration within the volume of this field. The performance of the focal length, the principal planes and the back focus are discussed in detail, the latter being of great significance with respect to perfect image formation at high magnification. For thin lenses an approximation leads to a concise formulation which is in accord with published experiments.

1. INTRODUCTION.

Many of the field lenses applied in electronic or ionic instruments make use of the focusing properties of cylindrical gaps or circular apertures or their equivalents arranged between magnetic poles or in electrostatic electrodes. The mathematical description of the electric or magnetic fields of such devices is possible, but cumbersome. Moreover, the solutions do not allow for an explicit determination of the actual electron trajectories. The electronic properties of the lenses, therefore, either must be derived by graphical or experimental methods, both of moderate accuracy and applicable to lenses of given parameters only, or they must be deduced from a consideration of the paraxial rays, necessitating methods of successive approximation. Other restrictions frequently applied for making a mathematical treatment possible are that the lenses be thin or weak, both excluding the most interesting case of small focal length.

In this paper we shall investigate the electronic properties of a field structure which will be developed directly from the postulate of electron focusing. Its field lines and equipotential surfaces are easy to survey and can be produced by appropriate mechanical and electrical means. The field is elementary in structure, and thus leads easily to an analytical

* Paper read at the Philadelphia meeting of the Electron Microscope Society of America on December 11, 1947. The investigation was originally made for the Farrand Optical Co., Inc., New York.

[1] Gordon McKay Professor of Electrical Engineering, Graduate School of Engineering, Harvard University, Cambridge, Mass.

determination of the electron trajectories. Therefrom the electron-optical performance can be derived, resulting in rigorous expressions for all the principal properties of the lens field. No aberrations of uniform electron rays occur within the formative volume of this field; such aperture defects are confined rather to the boundaries of the lens.

This analysis gives a direct insight into the details of ray-focusing and image-formation. It allows for correlation of the final results to the individual electron paths traversing the various parts of the field. Thus it permits us to visualize the performance of the lens better than do integral methods frequently used for such purposes.

By emphasizing the dependence of the field upon the radius as of the same importance as its dependence along the axis, we consider every element of the active space as equally significant. This method allows the development of a closed formulation for the cardinal points and for the lens aberrations, thus leading the way to a scientific design of electron lenses in contrast to the trial and error method often used heretofore.

Although such fields can be produced either by use of electrostatic electrodes or of magnetic poles, only the electrostatic case shall be considered here in detail. We limit ourselves in this paper further to the consideration of symmetrical converging fields. Diverging and accelerating fields may be treated in a following paper. No restrictions will be made as to paraxial rays or to thin or weak lenses. However, we shall exclude the consideration of space charge and of relativity effects, both being well-known by themselves for many types of electron beams.

2. FIELD STRUTURE.

Let us start with a short survey of the mathematical requirements for the electron lens fields. The analytical relations between field strength, potential and stream-function in a field of circular symmetry were developed by G. G. Stokes (1)[2] in 1842, and were first applied to hydrodynamic problems. In cylindrical coordinates r, z, the radial and axial components of the field strength $\mathcal{E}$ can be derived from a potential-function Φ by

$$\mathcal{E}_r = -\frac{\partial \Phi}{\partial r}; \qquad \mathcal{E}_z = -\frac{\partial \Phi}{\partial z}. \tag{1}$$

The same components may be derived also from a stream-function Ψ by

$$\mathcal{E}_r = \frac{1}{r}\frac{\partial \Psi}{\partial z}; \qquad \mathcal{E}_z = -\frac{1}{r}\frac{\partial \Psi}{\partial r}. \tag{2}$$

Potential and stream-function thus are interrelated by

$$\frac{\partial \Psi}{\partial r} = r\frac{\partial \Phi}{\partial z}; \qquad \frac{\partial \Psi}{\partial z} = -r\frac{\partial \Phi}{\partial r}. \tag{3}$$

[2] The boldface numbers in parentheses refer to the references appended to this paper, see Part II.

The field strengths of Eqs. 1 satisfy the condition of irrotationality

$$\frac{\partial \mathcal{E}_r}{\partial z} - \frac{\partial \mathcal{E}_z}{\partial r} = 0, \tag{4}$$

while the field strengths of Eqs. 2 satisfy the condition of continuity

$$\frac{\partial (r\mathcal{E}_r)}{\partial r} + \frac{\partial (r\mathcal{E}_z)}{\partial z} = 0. \tag{5}$$

On the other hand, Eqs. 1 substituted into Eq. 5 yield the differential equation which the potential-function must satisfy

$$\left.\begin{aligned} &\frac{\partial^2 \Phi}{\partial z^2} + \frac{1}{r}\frac{\partial}{\partial r}\left(r\frac{\partial \Phi}{\partial r}\right) = 0; \\ \text{or} \quad &\frac{\partial^2 \Phi}{\partial z^2} + \frac{1}{r}\frac{\partial \Phi}{\partial r} + \frac{\partial^2 \Phi}{\partial r^2} = 0, \end{aligned}\right\} \tag{6}$$

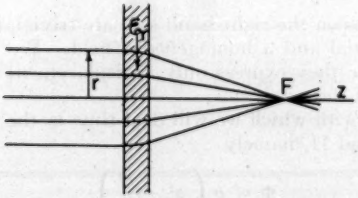

FIG. 1. Condition for focus formation.

and Eqs. 2 substituted into Eq. 4 yield the differential equation for the stream-function

$$\left.\begin{aligned} &\frac{\partial^2 \Psi}{\partial z^2} + r\frac{\partial}{\partial r}\left(\frac{1}{r}\frac{\partial \Psi}{\partial r}\right) = 0; \\ \text{or} \quad &\frac{\partial^2 \Psi}{\partial z^2} - \frac{1}{r}\frac{\partial \Psi}{\partial r} + \frac{\partial^2 \Psi}{\partial r^2} = 0. \end{aligned}\right\} \tag{7}$$

Equations 6 and 7 are by no means of identical form as they would be with two-dimensional problems.

If by action of a field lens the rays of a parallel electron beam of homogeneous velocity are to be deflected to converge toward or diverge from a point-focus on the axis of the beam, as shown in Fig. 1, the necessary condition is that the radial field strength, deflecting the electrons, is proportional to the radius

$$\mathcal{E}_r = p \cdot r. \tag{8}$$

In general, p might be a function of the axial coordinate z, but here we will consider p as a constant, characteristic for the strength of the lens-forming field. We will denote p as the power of the field.

Hence, the potential must contain a component as integrated from Eq. 1

$$\Phi' = -\int \mathcal{E}_r dr = -p\int r dr = -p\frac{r^2}{2} \tag{9}$$

to which an arbitrary constant or a function of z may be added. The actual dependence of the potential upon z can be determined by Eq. 6, as

$$\frac{\partial^2\Phi}{\partial z^2} = -\frac{1}{r}\frac{\partial}{\partial r}\left(r\frac{\partial}{\partial r}\left(-p\frac{r^2}{2}\right)\right) = 2p. \tag{10}$$

Two-fold integration with respect to z gives a second component of the potential

$$\Phi'' = \int dz\int 2p dz = z^2 + az + b. \tag{11}$$

The two last terms on the right-hand side are trivial, indicating merely a constant potential and a homogeneous field. We will not consider them further since they express only a displacement of the entire field in the direction of the z-axis.

The potential with which we will deal thus is the sum of the main terms in Eqs. 9 and 11, namely

$$\Phi = p\left(z^2 - \frac{r^2}{2}\right). \tag{12}$$

The factor p determines the power, the function of z and r the structure of the electromagnetic field, which shall be used here for the purpose of forming an electron lens.

The stream-function can be derived by integration of one of the Eqs. 3, yielding generally

$$\Psi = \int r\frac{\partial(\Phi' + \Phi'')}{\partial z}dr = \int r(2pz + a)dr = pzr^2 + a\frac{r^2}{2}. \tag{13}$$

With exclusion of the trivial last term, indicating merely a parallel flow, the stream-function is

$$\Psi = pzr^2. \tag{14}$$

Equations 12 and 14 indicate that in a meridian plane of z and r the stream lines, Ψ = constant, are cubic hyperbolas, while the equi-potential lines, Φ = constant, are ordinary hyperbolas, having a saddle-point at the origin $r = 0$, $z = 0$. The two families of curves are shown in Figs. 2 and 3. They are symmetrical to the origin. In the three-dimensional field of rotational symmetry around the z-axis, these

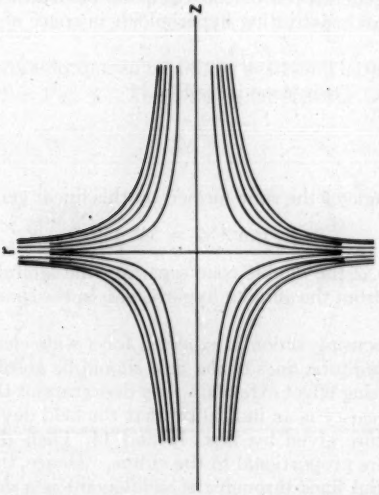

FIG. 3. Field lines, Ψ = constant, in hyperbolic lens.

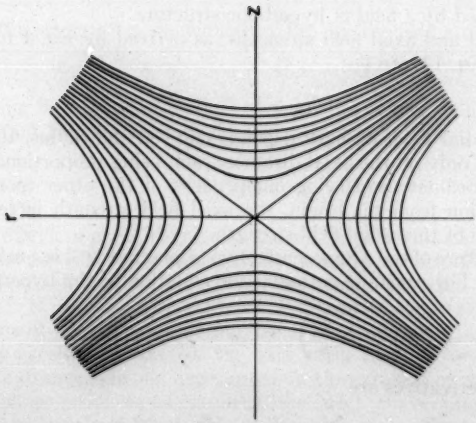

FIG. 2. Equipotential hyperboloids, Φ = constant, of lens field.

curves are the generatrices of the equipotential surfaces and of the stream tubes, both constituting hyperboloids in space of the order just mentioned.

The equipotential lines have rectilinear asymptotes given by the zero potential, $\Phi = 0$. Their slope is by Eq. 12

$$\frac{r}{z} = \sqrt{2}. \tag{15}$$

Thus the apex angle of the cone formed by this linear generatrix is

$$\alpha = \tan^{-1}\sqrt{2} = 54° 44'. \tag{16}$$

According to Fig. 2 the double cone separates the lateral hyperboloids within the cones from the annular hyperboloids in the space between the cones.

If a perfect focusing action is expected for a wide electron beam as in Fig. 1, the asymptotic lines of the field should be absolutely straight as far as the focusing effect extends. Any departure of the zero potential lines from linearity is an indication that the field deviates from the hyperbolic structure given by Eqs. 12 and 14. Then the radial field strength is no more proportional to the radius. Hence, the straightness of the equipotential lines through the saddlepoint is a criterion of the quality of the field structure.

Whereas in the case of light-optics, spherical or elliptical lenses can focus sharply a light beam of considerable radial extension, it appears that a uniform electron beam of substantial radial extension will be sharply focused by a field of hyperbolic structure.

The radial and axial field strengths, as derived by Eq. 1 from the potential of Eq. 12, are

$$\mathfrak{E}_r = pr; \qquad \mathfrak{E}_z = -2pz. \tag{17}$$

Thus, the radial field strength depends only on the radius, the axial field strength only on the axial distance, each being proportional to its respective coordinate and being independent of the other coordinate. With separation from the origin, the axial field strength increases at twice the rate of the radial field strength.

The curvature of the equipotential hyperbolas in Fig. 2 is a maximum at the axes. For constant potential the equation of the hyperbolas is

$$r = \sqrt{2\left(z^2 - \frac{\Phi}{p}\right)}; \quad \text{or} \quad z = \sqrt{\frac{\Phi}{p} + \frac{r^2}{2}}. \tag{18}$$

The second derivatives are

$$\frac{d^2r}{dz^2} = -2\frac{2z^2 - r^2}{r^3}; \qquad \frac{d^2z}{dr^2} = \frac{2z^2 - r^2}{4z^3} \tag{19}$$

and, therefore, the radii of curvature on the r-axis and on the z-axis are

$$\rho_r = \frac{r}{2}; \qquad \rho_z = 2z, \tag{20}$$

as represented in Fig. 4. Thus, for equal distance from the origin the

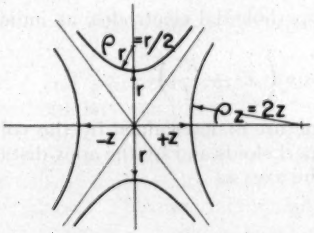

FIG. 4. Radii of curvature of equipotential hyperboloids.

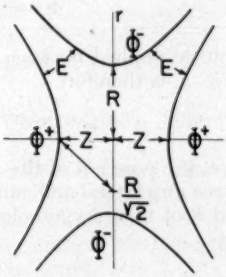

FIG. 5. Electrical and geometrical parameters of hyperbolic field.

annular hyperboloids are curved four times as much as the lateral hyperboloids.

The total field strength at any point of the field is

$$\mathcal{E} = \sqrt{e_r^2 + e_z^2} = p\sqrt{r^2 + (2z)^2}. \tag{21}$$

Along the asymptotes, as defined by Eq. 15, the field strength is

$$\mathcal{E}_a = \sqrt{3}pr = \sqrt{6}pz = \sqrt{2}pa, \tag{22}$$

increasing linearly with distance a from the origin. Thus the curves of constant field strength, as derived from Eq. 21, are

$$r^2 + (2z)^2 = \left(\frac{e}{p}\right)^2. \tag{23}$$

In the meridian plane they are ellipses of an axis-ratio 2:1.

If the power p of the field is chosen positive, the radial field strength from Eq. 17, is positive throughout the field. The axial field strength, however, is negative for positive z and positive for negative z. Thus electrons of negative charge moving through the field are throughout radially accelerated towards the axis, while axially they are retarded on the entrance side and accelerated on the exit side of the field. This performance produces an excellent lens effect, converging the electrons to a focus from whichever side they may come. A negative constant p, however, would diverge a stream of electrons away from the axis.

For positive p, the lateral hyperboloids, intersecting the z-axis at the distance Z for $r = 0$, as indicated in Fig. 5, have positive potential Φ^+ on both sides of the field. The annular hyperboloids, on the other hand, intersecting the r-axis at R for $z = 0$ have negative potential Φ^- throughout. Thus, the potentials are given by Eq. 12 as

$$\Phi^+ = pZ^2; \qquad \Phi^- = -p\frac{R^2}{2}. \tag{24}$$

A voltage applied between such hyperboloidal electrodes, as indicated by Fig. 5, is therefore

$$E = \Phi^+ - \Phi^- = p\left(Z^2 + \frac{R^2}{2}\right). \tag{25}$$

Hence, the power p of the field structure is determined by the voltage between any lateral and annular hyperboloids and by the apex distances Z and R of these hyperboloids on the axes as

$$p = \frac{E}{Z^2 + R^2/2}. \tag{26}$$

The denominator can be represented by a line from the end of Z to $R/\sqrt{2}$, as shown in Fig. 5.

The power p of the field is expressed by a magnitude of the dimension "volts per square centimeter," as distinguished from the dimension "volts per centimeter" of the field strength $\mathcal{E}$. Substitution of Eq. 26 into Eq. 21 or 22 permits the determination of the field strength at any place for given geometry and voltage between the electrodes.

3. ELECTROSTATIC TRAJECTORIES.

Since a field of hyperbolic structure, as described by Eqs. 12 and 14, develops field strengths, the components of which depend only on their own coordinates, see Eq. 17, the equations of motion of electrons through the field are extremely simple.

We consider converging lens fields of positive constant p. For electrons of mass m and charge $-q$, Newton's law is

$$m\frac{dv}{dt} = -q\mathcal{E}. \tag{27}$$

This yields, with the axial and radial components of velocity

$$v_r = \frac{dr}{dt}; \qquad v_z = \frac{dz}{dt} \tag{28}$$

and with use of Eq. 17,

$$\frac{d^2r}{dt^2} + \frac{q}{m}pr = 0; \qquad \frac{d^2z}{dt^2} - 2\frac{q}{m}pz = 0. \tag{29}$$

These are ordinary linear differential equations, separated in r and z. Their solution for the radial position of the electron is

$$r = A \cos(\nu t - \varphi); \qquad \nu = \sqrt{\frac{q}{m} p} \tag{30}$$

and for the axial position

$$z = B \sinh \mu t + C \cosh \mu t; \qquad \mu = \sqrt{2 \frac{q}{m} p}. \tag{31}$$

A, B, C and φ are constants of integration which must be determined by the boundary conditions.

We realize that radially the electrons perform ordinary sinusoidal oscillations about the z-axis with frequency ν, while axially the movement will be unilaterally retarded or accelerated on either side of the center plane. The time factor μ of the latter motion is related to the radial frequency ν of the former motion by the simple ratio

$$\frac{\mu}{\nu} = \sqrt{2}, \tag{32}$$

both parameters being determined solely by the power p of the field and by the ratio of charge to mass of the electrons. Hence, the motions of the electrons will be isochronous.

Let us first consider the sinh-solution of the electron rays with $C = 0$ in Eq. 31. In order to obtain the orbital equation, we eliminate the time from Eqs. 30 and 31. This yields with use of Eq. 32,

$$\left.\begin{aligned} \frac{r}{A} &= \cos\left[\frac{1}{\sqrt{2}} \sinh^{-1}\left(\frac{z}{B}\right) - \varphi\right]; \\ \text{or} \\ \frac{z}{B} &= \sinh\left[\sqrt{2}\left(\cos^{-1}\left(\frac{r}{A}\right) + \varphi\right)\right]. \end{aligned}\right\} \tag{33}$$

Both these equal expressions for the electron trajectories show that the radial amplitude A about the axis does not play any role for the shape of the curve. Only the ratio of radial distance r to amplitude A enters the equations. Therefore, the trajectories of different amplitudes, but of the same phase angle φ, are all of identical character. This indicates that all such trajectories intersect the z-axis at exactly the same points. These points are focal points of the electron rays. Hence this hyperbolic lens field does not produce any aberration with respect to the amplitude of the individual rays.

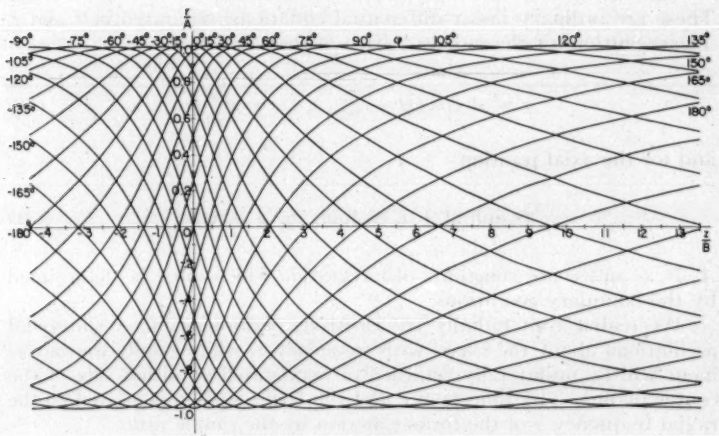

FIG. 6. Electron trajectories in hyperbolic lens field.

In Fig. 6 the entire family of trajectories for various phase angles φ is plotted, the variables being taken as r/A and z/B. The chart is extended on the right-hand side to larger values of z/B. If we follow from a point, as marked on the left-hand side of Fig. 7, the course of two of the trajectories taken from Fig. 6 and intersecting at this point, we see that they will intersect again on the right-hand side at a point

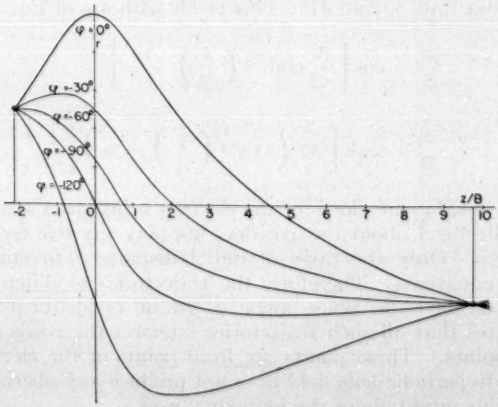

FIG. 7. Rays between conjugate image points.

the same distance from the axis as the point of origin. The same holds true for any two corresponding intersections of Fig. 6.

The two extreme traces in Fig. 7 belong to $\varphi = 0$ and $\varphi = -120°$. Three other trajectories are shown, belonging to $\varphi = -30°$, $-60°$ and $-90°$. These are reduced from Fig. 6 in amplitude in order to originate from the same point as marked on the left-hand side. They all join at the same intersection on the right-hand side, thus showing graphically that electron rays emerging from any point on the left-hand side unite at a common point on the right-hand side of the field, these conjugate points having the same distance from the axis. Hence, any pattern in a plane on the left-hand side of the origin can be imaged free of aberration and to scale on the right-hand side, and vice versa.

The value of the phase angle φ determines the position of the maxima and of the zero passages of the trajectories, as seen by Fig. 6. $\varphi = 0$ gives the ray of symmetry about the center plane, cutting the axis at the points

$$\pm \frac{z}{B} = \sinh\left(\sqrt{2}\,\frac{\pi}{2}\right) = 4.55. \tag{34}$$

$\varphi = \pm 90°$ gives the central rays traversing the axis at the center plane and reaching their amplitudes at the axial distances of Eq. 34.

We see that this family of trajectories constitutes an ideal field of rays, securing a perfect imaging of one radial plane to another, without, however, producing either magnification or reduction of the scale. The fact that the trajectories are compressed near the center plane and are expanding with separation from this plane is due to the increase of the axial field strength with axial distance, retarding or accelerating the electrons more and more, as determined by Eq. 31.

An electron beam consisting of parallel rays of homogeneous velocity entering the field structure at any radial plane, will be continued within the field structure by trajectories of various amplitudes, all having the same phase angle φ as determined by the plane of incidence. All these rays will be focused at a point on the axis which may lie on the left-hand side, in the center plane, or on the right-hand side, depending on the value of the phase angle φ at the plane of incidence.

The trajectories have points of inflection at regions where the axial field strength increases more than the radial field strength decreases. In order to obtain a relatively short focal distance of the trajectories, the field should not extend axially too far from the center plane since for large z the rays are converging very slowly.

If we express the trajectories, Eqs. 33, in the form

$$\varphi = \frac{1}{\sqrt{2}} \sinh^{-1}\left(\frac{z}{B}\right) - \cos^{-1}\left(\frac{r}{A}\right) \tag{35}$$

and note that the inverse cosine is double-valued, we realize that emerging from any point given by r/A and z/B there will develop two trajectories with different angles φ. These curves will proceed independently with changing z/B but will reach uni-valued points again for r/A equal in magnitude to that of the original point, but alternating in sign. By this mechanism of the trajectories, as illustrated by Figs. 6 and 7, electrons leaving any point within the field will meet again at an infinite number of points which are alternately above and below the z-axis. Hence there exist an infinite number of conjugate points and planes to the left and to the right, each forming a real image of all the others at a magnification ratio $\pm 1:1$. If z extends to great distances, or if B is small, the electrons oscillate many times during their transmission through the field. This is indicated in Fig. 8, where one of the trajectories is traced up to greater values of z/B.

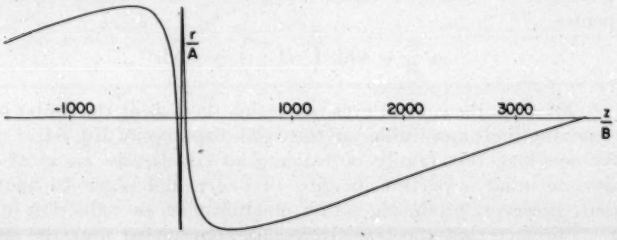

FIG. 8. Multiple oscillations of trajectory.

The velocity of the electrons in the radial direction is, by Eqs. 28 and 30,

$$v_r = -\nu A \sin(\nu t - \varphi) \tag{36}$$

and in the axial direction, by Eqs. 28 and 31,

$$v_z = \mu B \cosh \mu t. \tag{37}$$

Eliminating t from Eqs. 30 and 36, the radial velocity becomes

$$\frac{v_r}{\nu A} = -\sin\left(\cos^{-1}\left(\frac{r}{A}\right)\right) = \sqrt{1-\left(\frac{r}{A}\right)^2}. \tag{38}$$

This is mainly dependent on the radius r and graphically would form a circle diagram. The axial velocity, by elimination of t from Eqs. 31 and 37, is

$$\frac{v_z}{\mu B} = \cosh\left(\sinh^{-1}\left(\frac{z}{B}\right)\right) = \sqrt{1+\left(\frac{z}{B}\right)^2}. \tag{39}$$

This is dependent essentially on the axial distance z, and is given by a hyperbola, as indicated in Fig. 9.

Hence, on the left-hand side of the center plane the entering electrons are retarded to a minimum velocity which at $z = 0$ is

$$v_{z\,\min} = \mu B, \tag{40}$$

while on the right-hand side the electrons are accelerated to high velocities again. At considerable distances off the center plane the velocity changes nearly linearly with z, corresponding to the asymptotes of the hyperbolic velocity diagram in Fig. 9.

The radial and axial velocity components on the electron paths are independent of each other, see Eqs. 38 and 39, each being determined merely by its own coordinate, r or z. This independence is due to the fact that the potential Φ of the field does not contain any product of r and z, or product of functions of r and z. On the other hand, in an

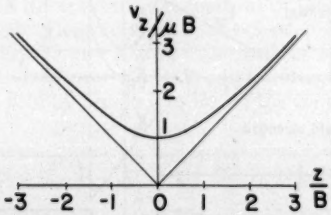

FIG. 9. Axial velocity distribution in lens field.

electromagnetic field having such product-structure, the differential equations for the coordinates of the electron paths, and still more the velocity components, would not be independent of each other. Therefore the formulation for the trajectories and for the velocities would be much more involved, rendering extremely difficult a rigorous analytical determination of the electronic qualities of the lens field.

4. TRANSMISSION CONSTANT.

In Fig. 10(a) is shown a beam of parallel electrons leaving an emitting cathode, which may have any negative potential, and entering a hyperbolic field at a distance $-Z$ from the origin. The electrons leave the field at a distance $+Z$ from the center, the field thus forming a symmetrical electron lens. While passing through the field, the electrons will follow the trajectories of Fig. 6, and therefore will converge towards a focus which may lie within or without the range of the lens field. Figure 10(b) shows the change of potential along the z-axis. The potential increases between the emitting cathode and the left-hand anode of the lens by a voltage E_V, constituting the accelerating voltage

of the electrons, or the velocity-voltage of the electrons entering the field. Within the lens space the potential changes parabolically, reaching a minimum 0 at the center. On the right-hand side externally to the lens field, the potential may be constant. Outside of the axis, the distribution of potential departs from that on the axis, as given by Eq. 12. The lower curve in Fig. 10(*b*) shows the distribution at the radius $r = R$. The voltage between the lateral equipotential hyperboloids, passing through axial points $\pm Z$, and the annular equipotential hyperboloid, passing through radial points R, again is denoted by E.

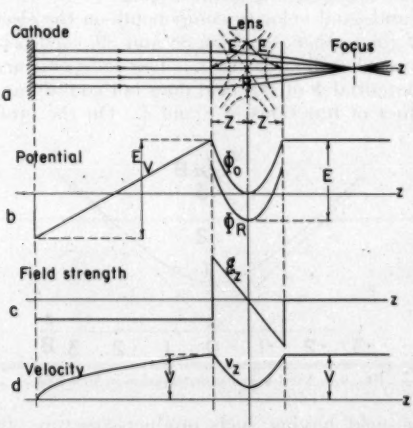

FIG. 10. Boundary conditions of a symmetrical lens.

Figure 10(*c*) shows the distribution of the axial field strength $\mathcal{E}_z$ along the axis, changing linearly within the lens space and, in our scheme, jumping at the boundaries to the field strength just outside of the lens space. Figure 10(*d*) shows the distribution of the axial electron velocity, having a value V at the entrance into the lens field. Within the lens the velocity varies hyperbolically with distance, attaining a minimum value at the center plane and again reaching the original velocity V on exit from the lens field.

In terms of the velocity voltage E_V of any incident electron considered, the entrance and exit velocity is given by

$$V = \sqrt{2\frac{q}{m}E_V}. \tag{41}$$

Within the lens, the axial velocity at the boundaries $\pm Z$ is given by Eq. 39 as

$$v_z = \mu\sqrt{B^2 + Z^2}. \tag{42}$$

Equating the last two expressions and substituting μ from Eq. 31, gives

$$E_V = p(B^2 + Z^2) \tag{43}$$

and therefrom the integration constant of the ray can be determined as

$$B = \sqrt{\frac{E_V}{p} - Z^2} = \sqrt{\left(\frac{V}{\mu}\right)^2 - Z^2}. \tag{44}$$

The last expression contains the entrance velocity V rather than the incident velocity voltage E_V.

If in the lens space the initial distribution of the axial velocity over the cross section of the beam is uniform, it remains uniform throughout the lens field. We will consider here this condition as being fulfilled, although it may require special arrangements to secure this performance of the electron beam when entering the lens field. A later section of this paper will deal with the deviations if this condition is not satisfied.

We denote B as the transmission constant of the lens-ray arrangement because its value determines the axial development of the trajectories as seen by Eq. 33 and Fig. 6. The smaller B is, the more the trajectories are refracted over a certain axial distance z. Substituting the power p of the field by Eq. 26 into Eq. 44 the transmission constant becomes

$$B = \sqrt{\frac{E_V}{E}\left(Z^2 + \frac{R^2}{2}\right) - Z^2} = \sqrt{\left(\frac{E_V}{E} - 1\right)Z^2 + \frac{1}{2}\frac{E_V}{E}R^2}. \tag{45}$$

The dimension of this constant is centimeters.

We see from the right-hand side of Eq. 45 that the transmission constant depends on three parameters only, namely: the half-thickness Z of the lens, the radius R of the central aperture, and the ratio of the velocity voltage E_V of the incident electrons to the lens voltage E between the hyperboloids through Z and R.

With increasing lens voltage E, the transmission constant B decreases, becomes zero and finally imaginary. In these latter cases the lens loses its ability to transmit electrons. Hence, the condition for transmission of an electron beam is, that the lens voltage with respect to the incident electron voltage must be smaller than

$$\left(\frac{E}{E_V}\right)_0 = 1 + \frac{1}{2}\left(\frac{R}{Z}\right)^2, \tag{46}$$

a ratio which is plotted in Fig. 11 as depending on the relative lens thickness Z. For larger lens voltage or smaller electron voltage than is determined by this condition, the potential in the center of the field would be lower than that of the cathode, and therefore no electrons could pass through the lens. Thus, Eq. 46 determines the blocking voltage of the lens.

When approaching this blocking condition, the transmission constant B becomes very small. Then the electrons will perform an increasing number of radial oscillations within the lens volume, as shown by Fig. 8.

If the annular electrode of the lens is directly connected to the emitting cathode, the lens voltage is $E = E_V$, and the transmission constant becomes by Eq. 45

$$B = \frac{R}{\sqrt{2}}. \tag{47}$$

Hence, for a unipotential lens the transmission constant is independent of the thickness Z of the lens and solely determined by R.

For short lenses Z is relatively small and for weak lenses E_V/E is relatively large, both cases leading to a similar simplification of Eq. 45.

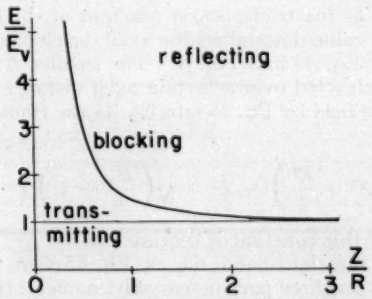

FIG. 11. Blocking voltage *versus* lens thickness.

The use of these approximations, however, would not simplify the development of the further analysis in this paper.

In all cases where E is equal to or smaller than E_V, the lens will always transmit the electron beam, see Eq. 46. If, however, the lens voltage is higher than the incident electron voltage, the ratio Z/R determines whether the beam will be transmitted or blocked.

Figure 11 shows that with large half-width Z the blocking condition is reached at lower lens voltages than with large aperture-radius R. For $Z = R$ the blocking voltage is 1.5 times the incident velocity voltage of the electrons. In order to avoid a relatively unstable performance near the blocking condition, it is not advisable to operate at too large a ratio Z/R for unipotential lenses.

The minimum axial velocity, Eq. 40, to which the electron rays are reduced at the lens center, can be expressed by substitution of μ from

Eq. 31, of B from Eq. 44, and of p from Eq. 26 as

$$v_{z\,\min} = V\sqrt{1 - \frac{E/E_V}{1 + R^2/2Z^2}}. \tag{48}$$

This is plotted in Fig. 12 and shows that near the blocking condition of Eq. 46 the axial velocity in the center plane of the lens rapidly approaches zero.

In Fig. 6 the electron trajectories have been plotted as depending on an axial coordinate z/B. For actual examples it is convenient to convert this coordinate to a ratio z/Z which has a direct bearing on the physical width Z of the lens. This can be done by multiplying the variable z/B by a factor B/Z, the value of which, by Eq. 45, is

$$\frac{B}{Z} = \sqrt{\frac{E_V}{E}\left[1 + \frac{1}{2}\left(\frac{R}{Z}\right)^2\right] - 1}. \tag{49}$$

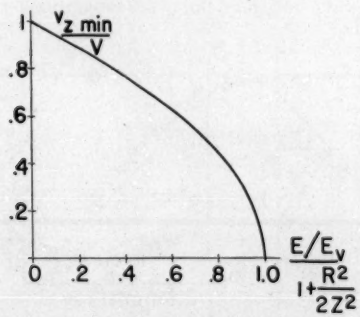

FIG. 12. Change of minimum velocity in lens center.

Table I gives some values of this ratio for a number of lens voltages and central lens apertures. We see that for such relations B is of the order of magnitude of the half-thickness of the lens. In the blank spaces the lens is blocking the beam.

TABLE I.—*Ratio B/Z of Transmission Constant to Half-Width of the Lens.*

E/E_V =	$\frac{1}{4}$	1	2
$\frac{R}{Z} = \frac{1}{2}$	$\frac{5}{4} = 1.12$	$\frac{1}{\sqrt{8}} = 0.354$	
$\frac{R}{Z} = 1$	$\sqrt{2} = 1.41$	$\frac{1}{\sqrt{2}} = 0.707$	
$\frac{R}{Z} = 2$	$\sqrt{5} = 2.24$	$\sqrt{2} = 1.41$	$\frac{1}{\sqrt{2}} = 0.707$

Now we can determine the characteristic frequencies ν and μ of the electron motion as in Eqs. 30 and 31. Substituting p from Eq. 26, and expressing q/m from Eq. 41, the frequency of the radial oscillations of the electrons is

$$\nu = \frac{V}{\sqrt{2Z^2 + R^2}}\sqrt{\frac{E}{E_V}}. \tag{50}$$

For a unipotential lens with $E = E_V$, an incident electron velocity of half the velocity of light, $V = 1.5 \cdot 10^{10}$ cm. per second corresponding to $E_V = 64$ kv., and dimensions $R = Z = 1$ cm., the frequency is

$$\frac{\nu}{2\pi} = \frac{1.5 \cdot 10^{10}}{2\pi\sqrt{2 \cdot 1^2 + 1^2}}\sqrt{1} = 1.38 \cdot 10^9 \text{ cps.}$$

Thus, for such an example, the frequency of ν, and also that of μ, will be of the order of thousands of megacycles, and the corresponding electromagnetic wave length of the order of centimeters.

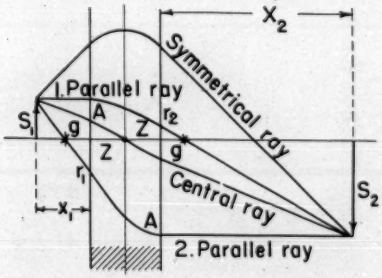

FIG. 13. Image formation by four principal rays.

Beyond the blocking condition of Eq. 46 the transmission constant B becomes imaginary and therefore the second solution of Eq. 31, with integration constant C, should be used. Since cosh has a minimum value of unity and has two branches of the same sign, the electrons now cannot reach $z = 0$, but will return on the second branch. Hence, whereas the first term of Eq. 31 represents a lens action, the second term indicates the action of a mirror.

8. CARDINAL POINTS.

We will consider four characteristic rays as indicated in Fig. 13, namely incident and emerging parallel rays, central rays, and symmetrical rays. The investigation of these significant rays transmitted through a hyperbolic field may stand for a more general analysis. We

suppose the lens field to be axially symmetrical, and to be limited by two radial planes at the distance $\pm Z$ from the center of the field.

Incident or emerging parallel rays in the external space are continued through the boundaries of the lens by rays within the field which have at $z = \pm Z$ the value $r/A = \pm 1$, as seen immediately from Fig. 6. Inserted into Eq. 33 this yields

$$\pm \frac{Z}{B} = \sinh\left[\sqrt{2}(0 + \varphi)\right]; \qquad \varphi = \pm \frac{1}{\sqrt{2}} \sinh^{-1}\left(\frac{Z}{B}\right), \tag{51}$$

thus determining the phase angles φ of the two parallel rays of Fig. 13.

The equations of these rays within the volume of the lens are given by inserting φ from Eq. 51 into the first Eq. 33

$$\frac{r}{A} = \cos\left[\frac{1}{\sqrt{2}}\left(\sinh^{-1}\left(\frac{z}{B}\right) - \frac{1}{\sqrt{2}} \sinh^{-1}\left(\frac{Z}{B}\right)\right)\right]. \tag{52}$$

For both of the parallel rays the abscissa z at the converging end of the ray in the lens is opposite in sign to the abscissa of the parallel end of the ray, $z = -Z$. Both sinh's in Eq. 52 then have the same magnitude and sign, yielding the radii at the converging ends of the rays as

$$\frac{r}{A} = \cos\left[\sqrt{2} \sinh^{-1}\left(\frac{Z}{B}\right)\right]. \tag{53}$$

We may ask for the condition that parallel incident rays will directly focus at the opposite boundary of the field. Then we have in Eq. 53, $r/A = 0$, giving with use of Eq. 51

$$\pm \sinh^{-1}\left(\frac{Z}{B}\right) = \frac{\pi}{2\sqrt{2}}; \qquad \frac{Z}{B} = 1.35; \qquad \varphi = \pm \frac{\pi}{4}. \tag{54}$$

It may be verified by Fig. 6 that parallel rays entering a symmetrical lens at $\varphi = -45°$, focus just at the other end at $\varphi = +45°$. In this case the thickness of the lens would be 90°, measured in units of φ.

Outside of the lens field the rays propagate linearly, with constant slope. Quite generally, the slope of the rays within the lens field, as given by differentiation of Eq. 33, is

$$\frac{dr}{dz} = -\frac{A}{B} \frac{\sin\left[\frac{1}{\sqrt{2}} \sinh^{-1}\left(\frac{z}{B}\right) - \varphi\right]}{\sqrt{2\left(1 + \left(\frac{z}{B}\right)^2\right)}}. \tag{55}$$

Introducing herein the value of the phase angle φ from Eq. 51 for parallel entrance of the ray at $-Z$, and the abscissa $z = +Z$ for the

converging exit, the slope of the ray leaving the lens is

$$\frac{dr}{dz} = -\frac{A}{B}\frac{\sin\left[\sqrt{2}\sinh^{-1}\left(\frac{Z}{B}\right)\right]}{\sqrt{2\left(1+\left(\frac{Z}{B}\right)^2\right)}}. \tag{56}$$

This ray intersects the axis at a distance g from the surface of the lens field, which length usually is denoted as back-focus and is given in Fig. 14 by the subtangent

$$g = \frac{r}{dr/dz}. \tag{57}$$

Substituting the numerator by Eq. 53 and the denominator by Eq. 56, the back-focus is

$$g = \frac{\sqrt{2}\,B\sqrt{1+\left(\frac{Z}{B}\right)^2}}{\tan\left[\sqrt{2}\sinh^{-1}\left(\frac{Z}{B}\right)\right]}. \tag{58}$$

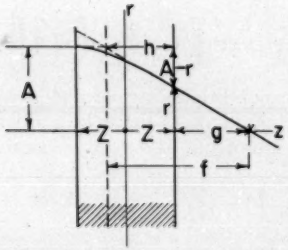

FIG. 14. Parallel incident ray and cardinal lens points.

This value is independent of the initial amplitude A, indicating that bundles of uniform parallel rays are refracted rigorously toward a point-focus, independent of the width of the incident beam. This shows again that the hyberbolic structure of the field is entirely free from aperture defects for uniform parallel beams.

Due to our supposition of a symmetrical field, the back-focus is the same for both sides of the lens. Its magnitude depends only on the transmission constant B and on the ratio of half-thickness Z to this constant B. Figure 15 shows the change of the back-focus with the lens thickness Z, both values taken as ratio to the transmission constant B. If the relative lens thickness Z/B increases from 0 to 4.55, the back-focus changes from $+\infty$ through 0 to $-\infty$.

If we express the main factors in the numerator of Eq. 58 in terms of the original lens parameters, we obtain with use of Eq. 45

$$B\sqrt{1+\left(\frac{Z}{B}\right)^2}=\sqrt{B^2+Z^2}=\sqrt{\frac{E_r}{E}\left(Z^2+\frac{R^2}{2}\right)}. \tag{59}$$

This is a characteristic length which will appear in many of the following equations, and which is given solely by the square root of the voltage ratio and the main dimensions of the hyperbolic lens.

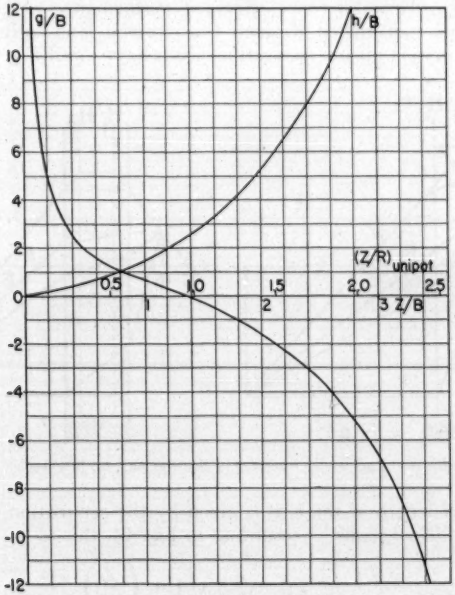

FIG. 15. Change of back-focus and principal plane with lens thickness.

The position of the principal plane, as shown in Fig. 14, is determined by the intersection of the entrance and exit tangents of the parallel ray. The distance of this point from the end of the lens is

$$h=\frac{A-r}{dr/dz}=B\sqrt{2\left(1+\left(\frac{Z}{B}\right)^2\right)}\,\frac{1-\cos\left[\sqrt{2}\,\sinh^{-1}\left(\frac{Z}{B}\right)\right]}{\sin\left[\sqrt{2}\,\sinh^{-1}\left(\frac{Z}{B}\right)\right]} \tag{60}$$

which transforms by a well-known trigonometric relation to

$$h = \sqrt{2}\, B \sqrt{1 + \left(\frac{Z}{B}\right)^2} \tan\left[\frac{1}{\sqrt{2}} \sinh^{-1}\left(\frac{Z}{B}\right)\right]. \tag{61}$$

The second curve in Fig. 15 shows the change of this value with lens width. We see that h is larger than Z, showing that for the emerging ray the principal plane in such electron lenses always is situated on the entrance side of the rays. This is in contrast to simple light optical lenses, where this principal plane for the most part is on the exit side of the rays. This difference effects a performance of the principal electron rays transmitted through the electron lens as in Fig. 16(a), while light rays in glass lenses ordinarily behave as in Fig. 16(b).

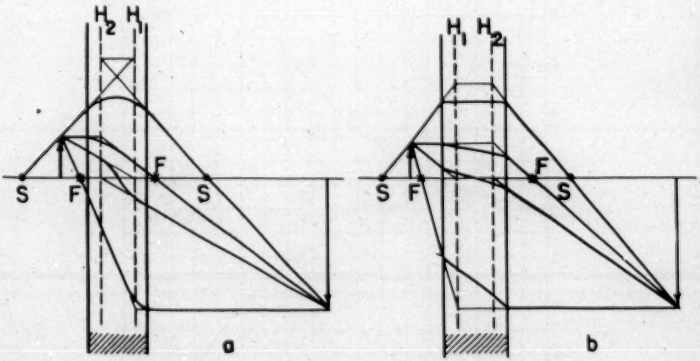

FIG. 16. Ray propagation, (a) in electron lens, (b) in glass lens.

The focal length of the lens is given by the separation of the focus from the principal plane. According to Fig. 14, this is

$$f = \frac{A}{dr/dz} = \frac{\sqrt{2}\, B \sqrt{1 + \left(\frac{Z}{B}\right)^2}}{\sin\left[\sqrt{2} \sinh^{-1}\left(\frac{Z}{B}\right)\right]}. \tag{62}$$

The ratio f/B is plotted in Fig. 17, giving large values for both thin and thick lenses. The focal-length ratio shows a marked minimum at the point

$$\frac{Z}{B} = 0.89; \qquad \frac{f}{B} = 2.08, \tag{63}$$

leading to $f = 2.35\, Z$ as optimum focal length with respect to the ratio Z/B of the half-width. However, the transmission constant B, to

which Z and f here are related, is in general dependent on Z, as given by Eq. 45.

Only for unipotential lenses is the constant B independent of Z as shown by Eq. 47. For such lenses the optimum length is

$$Z_{opt} = 0.63R \tag{64}$$

and the minimum focal length will be

$$f_{min} = 1.48R. \tag{65}$$

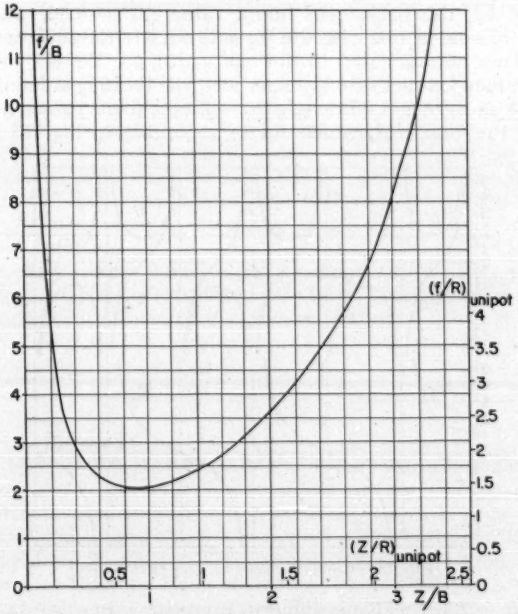

FIG. 17. Change of focal length with lens thickness.

In Fig. 17 the values are indicated which the coordinates assume in f/R and Z/R for a unipotential lens. For any other lens voltage the actual position and magnitude of the minimum of f are depending also on E/E_V and can be determined by supplementary differentiation of B from Eq. 45.

We see from Fig. 17 that axially thin lenses have a considerable focal length. This can be diminished either by greater thickness of the lens field, as given by Z, or by smaller transmission constant B, which is further determined by lens voltage E and radius R, see Eqs. 45 or 47.

Both changes lead to a greater effect of the field on the electrons. However, extending this effect beyond a certain limit will be of no avail since the focal length after passing through a minimum will rise again due to the decreasing slope of the trajectories in Fig. 6 with increasing Z/B.

By use of Eq. 62 and Fig. 17, such lenses can be readily designed with respect to voltage, width and aperture in order to obtain a desired focal length.

From the curve in Fig. 15 we see that for the minimum focal length, as in Eq. 63, the back-focus has a value $g/B = 0.86$, which is still positive. Thus, in this case the focus is outside the surface of the lens at a distance almost equal to the half-width, see Eq. 63. For thicker lenses the focus moves into the lens field, the limiting value being given by Eq. 54 as $Z/B = 1.35$. At $g = -Z$, the focus passes through the center of the lens field, which occurs according to Fig. 15 for a half-

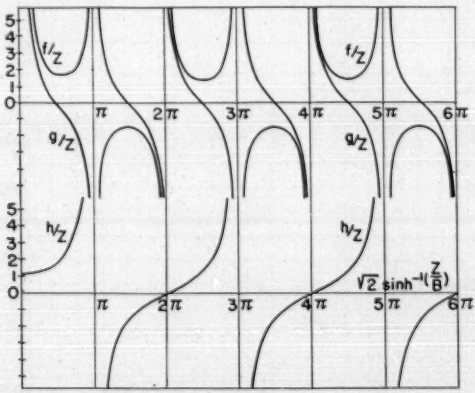

FIG. 18. Cardinal values for very thick lenses.

width $Z/B = 2.16$. This is different from the $\varphi = -90°$ trajectory of Fig. 6 starting parallel at $Z/B = -4.55$, since inside the lens Eq. 58 indicates the virtual position of the focus of the emerging rectilinear rays rather than the actual intersection of the trajectories.

For still thicker lenses, the position of the virtual focus, given by g, moves rapidly toward $-\infty$ on the incident side of the lens. The principal plane, however, determined by h, moves much faster to the same side, see Fig. 15. Thus, the focal length f, as separation of focus and principal point, finally is entirely to the far left of the lens field.

If we increase the lens width beyond the value $Z/B = 4.55$, the back-focus g, as determined by a trigonometric tangent, repeats moving

similar to Fig. 15. However the focal length f, as determined by a sine, now becomes negative and will change its sign repeatedly with further increase of Z. This indicates the formation of a diverging lens in the zones of negative sign. Figure 18 shows the performance of f, g, and h with greatly increasing ratio Z/B. The cardinal values are related here to Z rather than to B in order to yield more uniform curves; and as abscissa there is plotted the inverse sinh rather than its argument Z/B for the same reason. We see from Eq. 49 in combination with Eq. 46, that we are now close to the blocking condition and thus, such lenses will be somewhat sensitive.

It is interesting to see that, in principle, diverging lenses can be produced by the same technical means as converging lenses. From the trajectories of Fig. 6 it is clear that for formation of a diverging effect, the electrons must stay within the lens for more than one half a radial oscillation, thus converting the condensing action of the field into a diverging effect. For unipotential lenses, we derive from Eq. 47 that the width of the field must be $Z > 3.21R$. However, the minimum focal length will not occur before $Z = 10R$ and then has a value of $f = 1.42Z$. Hence, strongly diverging lenses must have a relatively small central aperture.

For lenses of greater width Fig. 18 indicates that alternately converging and diverging effects are produced. This behavior soon becomes periodic with respect to the abscissa shown.

For thin lenses we can develop Eq. 62 into a power series, the first two terms of which, with use of Eq. 45, are

$$f \cong \frac{B^2}{Z} + Z = \frac{E_v}{E}\left(Z + \frac{1}{2}\frac{R^2}{Z}\right). \tag{66}$$

Therefore, the focal length of a thin lens is parabolically dependent on the aperture and hyperbolically dependent on the thickness. For a thin unipotential lens with $E = E_v$, the focal length is always greater than the half-width, and there is a very simple relation with respect to the dimensions R and Z. This formulation may be used as an approximation also for other types of electron lenses and is in good accord with some experimental results (6) for three-plate-aperture lenses.

The last approximate formula (66) for the focal length, or even the former rigorous equations for all of the cardinal points, may be used to advantage if lenses of arbitrary field distribution are to be analysed or synthesized. The actual variation of the potential, paraxial and extra-axial, may be approximated by a number of potential fields as in Eq. 12 each forming an elemental lens of hyperbolic structure.

6. IMAGE FORMATION.

Let us now consider the formation of the image and the magnification of the object. If S_1 and S_2 are the magnitudes of object and image,

we see from Fig. 19 that the following geometrical relations hold between the distances x from the lens surfaces and the back-focus g: For the object space

$$\frac{x_1}{g} = \frac{S_1 + r_1}{r_1} = \frac{S_1}{S_2 \cos\left[\sqrt{2}\sinh^{-1}\left(\frac{Z}{B}\right)\right]} + 1 \qquad (67)$$

and for the image space

$$\frac{x_2}{g} = \frac{S_2 + r_2}{r_2} = \frac{S_2}{S_1 \cos\left[\sqrt{2}\sinh^{-1}\left(\frac{Z}{B}\right)\right]} + 1. \qquad (68)$$

On the right-hand sides of both equations we have substituted Eq. 53 for the ratios of exit radius and entrance amplitude of a parallel incident ray, the radii being r_1 and r_2 and the amplitudes being S_2 and S_1.

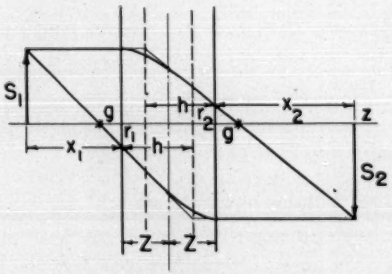

FIG. 19. Image formation by parallel rays.

By multiplying the first terms of the right-hand sides of Eqs. 67 and 68, the S-ratios cancel and there remains

$$\frac{g^2}{\cos^2\left[\sqrt{2}\sinh^{-1}\left(\frac{Z}{B}\right)\right]} = (x_1 - g)\cdot(x_2 - g). \qquad (69)$$

Substituting now g from Eq. 58 and using f from Eq. 62 yields

$$f^2 = (x_1 - g)(x_2 - g). \qquad (70)$$

This is Newton's formula, correlating the focal length and the distances of object and image from the respective focal points, see Fig. 19. By purely geometrical means this formulation can be transformed into

$$\frac{1}{f} = \frac{1}{x_1 + h} + \frac{1}{x_2 + h}, \qquad (71)$$

where h is the principal distance, according to Eq. 61. Thus, a hyperbolic electron lens behaves, with respect to the distances of object and image, like a perfect light-optical lens.

By dividing the first terms of the right-hand sides of Eqs. 67 and 68, the cosines cancel and there results

$$\left(\frac{S_2}{S_1}\right)^2 = \frac{x_2 - g}{x_1 - g}, \tag{72}$$

yielding the magnification ratio, also in Newton's form. This can be transformed by purely geometrical manipulation into the conventional form

$$\frac{S_2}{S_1} = \frac{x_2 + h}{x_1 + h}. \tag{73}$$

Thus, a hyperbolic electron lens behaves also with respect to the magnification like a perfect light-optical lens. For many practical applications of electron lenses, Eqs. 70 and 72 are more convenient to use than

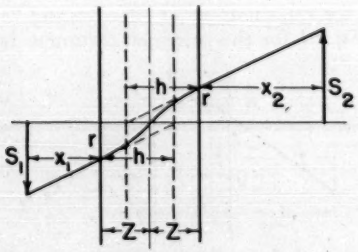

FIG. 20. Image formation by central ray.

the conventional Eqs. 71 and 73. They show that, particularly for high magnification, the back-focus g rather than the focal length f plays the dominant role in precise image formation.

So far we have derived the performance of the lens from the two parallel rays transmitted through the field. It is interesting to see that use of the central ray, as shown in Fig. 20, will lead to identical results. For this ray the phase angle is $\varphi = \pm 90°$, as in Fig. 6, and thus the trajectories are given by the first Eq. 33 as

$$\frac{r}{A} = \pm \sin\left[\frac{1}{\sqrt{2}} \sinh^{-1}\left(\frac{z}{B}\right)\right]. \tag{74}$$

The slope at the entrance and exit of the lens field is, from Eq. 55,

$$\frac{dr}{dz} = \frac{A}{B} \frac{\cos\left[\frac{1}{\sqrt{2}} \sinh^{-1}\left(\frac{Z}{B}\right)\right]}{\sqrt{2\left(1 + \left(\frac{Z}{B}\right)^2\right)}}, \tag{75}$$

having the same sign for positive and negative Z.

The magnitudes of object and image are given, as in Fig. 20, by the sums of the entrance or exit radius r and the elevation above the distance x from the lens surface

$$S_1 = r + x_1\left(\frac{dr}{dz}\right); \qquad S_2 = r + x_2\left(\frac{dr}{dz}\right). \tag{76}$$

Thus, the magnification is

$$\frac{S_2}{S_1} = \frac{x_2 + \frac{r}{dr/dz}}{x_1 + \frac{r}{dr/dz}} = \frac{x_2 + h}{x_1 + h}, \tag{77}$$

wherein h stands for the quotient of Eqs. 74 and 75. This, however, is identical with Eq. 61 for the principal distance, and thus we are led

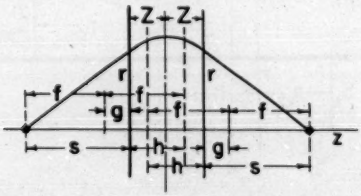

FIG. 21. Image formation by symmetrical ray.

to the conventional value of the magnification. We see further from Eq. 77 and Fig. 20 that the tangents to the central ray intersect the axis at the principal points given by the distance h from the lens surface. Hence, the central ray participates correctly in the image formation of the object.

The same can be shown for the symmetrical ray, as indicated in Fig. 16, or for any other ray. It may be noted, however, that the straight line diagram for the fictitious path of the symmetrical electron ray, as in Fig. 16(a), deviates considerably from the corresponding symmetrical path ordinarily assumed for light rays as in Fig. 16(b).

Instead of repeating the pattern of the last derivation, let us consider the intersection of the symmetrical ray with the axis as shown in

Fig. 21. At the lens surface the radius, with $\varphi = 0$ according to Fig. 6 and Eq. 33, is given by

$$\frac{r}{A} = \cos\left[\frac{1}{\sqrt{2}}\sinh^{-1}\left(\frac{Z}{B}\right)\right]. \tag{78}$$

The slope of the ray at the surfaces, by Eq. 55, is

$$\frac{dr}{dz} = \pm\frac{A}{B}\frac{\sin\left[\frac{1}{\sqrt{2}}\sinh^{-1}\left(\frac{Z}{B}\right)\right]}{\sqrt{2\left(1+\left(\frac{Z}{B}\right)^2\right)}}. \tag{79}$$

The ray intersects the axis at distances from the surfaces on both sides of the lens

$$s = \frac{r}{dr/dz} = B\sqrt{2\left(1+\left(\frac{Z}{B}\right)^2\right)}\cot\left[\frac{1}{\sqrt{2}}\sinh^{-1}\left(\frac{Z}{B}\right)\right]. \tag{80}$$

If we add to this focal distance s the depth h of the principal plane beyond the surface, see Eq. 61, we obtain after the common factor $B\sqrt{2\left(1+\left(\frac{Z}{B}\right)^2\right)}$ a sum which can be condensed to

$$\cot\left[\frac{1}{\sqrt{2}}\sinh^{-1}\left(\frac{Z}{B}\right)\right]+\tan\left[\frac{1}{\sqrt{2}}\sinh^{-1}\left(\frac{Z}{B}\right)\right]=\frac{2}{\sin\left[\sqrt{2}\sinh^{-1}\left(\frac{Z}{B}\right)\right]}. \tag{81}$$

Thus, the entire distance from principal point to focus is

$$s+h = 2\frac{\sqrt{2}\,B\sqrt{1+\left(\frac{Z}{B}\right)^2}}{\sin\left[\sqrt{2}\sinh^{-1}\left(\frac{Z}{B}\right)\right]} = 2f, \tag{82}$$

the quotient in the middle term being identical with the focal length of Eq. 62. Hence, every symmetrical ray, whatever its amplitude, cuts the axis on both sides at a distance of twice the focal length from the principal planes, or at a distance of focal length from the focus.

(*To be continued.*)

America's Most Powerful Aircraft Jet Engine in Production.—America's most powerful aircraft jet engine now in production, General Electric's torpedo-shaped TG-190, which is capable of producing approximately 10,000 hp. at the top speed of the new planes being built for its application, has been announced by the U. S. Air Force and the company's Aircraft Gas Turbine Divisions.

Known as the Air Force J-47A, the new engine is a "greatly advanced" development of the company's axial-flow TG-180 (J-35) jet engine which is the power plant of 10 different types of military jet-propelled fighters and bombers.

Although having approximately the same frame size as the TG-180, the TG-190 has many design improvements, a greater thrust rating and is substantially the same weight as the former unit. Compared with the slightly more than 4000-lb. thrust developed by the TG-180, the new engine has 25 per cent more power, according to the Air Force.

Future development of the TG-190 jet, according to engineers, promised to increase its rating to 6000-lb. thrust.

With a rating of approximately 5000-lb. thrust, which is equivalent to about twice as many horsepower under certain conditions, the TG-190 has been in production at the company's Lynn River, Mass., plant since the U.S.A.F. officially accepted the prototype in the fall of 1947. Engineers explained that "thrust" is a force, and the propulsive horsepower being developed depends upon the speed of the airplane. At an airplane speed of 375 miles an hour, one pound of thrust is equal to one horsepower of propulsive effort.

First units of the new engine have been undergoing extensive ground tests at the plant. Following completion of the military-required type-testing in the factory, the TG-190 now has been installed as the powerplant of the North American F-86A, an Air Force fighter recently revealed as having a speed of "over 650 miles an hour." The North American XF-86 now uses the General Electric-designed TG-180 jet engine.

Altitude and other tests with the new engine also have been underway aboard the B-29 flying laboratory operated by G.E. at its Flight Test Center near Schenectady, N. Y. As in the case of the TG-180, the TG-190 has been installed in the bomb bay of the Boeing Superfortress for flight testing under altitude conditions. The flying laboratory, operated by G-E engineers and manned by a Pan American crew, also is an Air Force project.

R. H. O.

Induction Heating Equipment Available Without Capital Investment.—For the first time, THER-MONIC Induction and Dielectric Heating equipment is made available to industry under a Rental-Purchase Plan. Under this plan, recently established by the Induction Heating Corporation, Brooklyn, N. Y., new or used (latter, when available) Induction or Dielectric Generators may be rented on a monthly basis with the option to buy at any time. A portion of rental payments forms an equity towards outright purchase.

This Rental-Purchase Plan is unique in the heavy equipment field in that it benefits the following—the manufacturer who insists upon "proof prior to purchase," the manufacturer who for some reason or other would rather not make an immediate capital investment and the manufacturer whose set-up is such as to prefer a continuing "pay-as-you-go" arrangement.

V.24
194

NOTES FROM THE NATIONAL BUREAU OF STANDARDS.*

THE EFFECT OF SCREENS IN WIND-TUNNEL WIDE-ANGLE DIFFUSERS.

Extensive experimental research under the direction of G. B. Schubauer and W. G. Spangenberg of the National Bureau of Standards has led to a more complete understanding of the effect of damping screens in wind-tunnel wide-angle diffusers.[1] Results have shown that the usual undesirable turbulence in such rapidly expanding ducts can be greatly reduced by suitable location of fine wire screens. Thus, wide-angle diffusers may now be utilized for increasing the cross section of an air stream within a very short length of travel.

A wind tunnel is designed to simulate, as nearly as possible, the motion of a body through still air by producing a smooth, uniform flow of air past the body. The air stream, drawn through a circuit of ducts by a propeller, is accelerated into the test section—the part of smallest cross-sectional area—through a nozzle or entrance cone. The greater the contraction ratio (ratio of the area of the larger end of the entrance cone to that of the smaller end) the less turbulent is the flow through the test section.

Recent wind-tunnel investigations at the Bureau have shown that damping screens [2] placed across the section upstream of the entrance cone are a very effective means for reducing turbulence in the test section of a tunnel. Whether screens are used or not, however, it is always desirable to have the contraction ratio as large as possible, and this has usually been accomplished in complete-circuit tunnels by making the return circuit of long, gradually expanding ducts known as narrow-angle diffusers.

A few years ago, it was observed that the cross section of an air stream could be increased in an unusually short length of travel through a rapidly expanding duct if the larger end of the duct was covered by a screen. This observation by members of the staff of the National Advisory Committee for Aeronautics was very significant, as years of experience had apparently shown that the only way an enclosed stream could be induced to increase its cross section uniformly was by means of a long, gradually expanding duct.

The conventional narrow-angle diffuser is a very long funnel-shaped tube with an included wall angle of about 8 deg. The term "wide-angle

* Communicated by the Director.

[1] Complete details of this work are described in NACA Technical Note No. 1610 by G. B. Schubauer and W. G. Spangenberg.

[2] Damping wind-tunnel turbulence, *NBS Technical News Bulletin*, 31, 1 (1947).

diffuser" is applied to ducts with walls diverging at much greater angles —for example, 30 deg., or perhaps even 90 deg. in extreme cases. If the transition from a smaller to a larger duct is made through a wide-angle diffuser, flow from the smaller to the larger duct ordinarily becomes very nonuniform because the air stream will not follow the walls of the diffuser. The flow may also whip from side to side and pulsate violently. These effects are summed up by saying that the diffuser fails to fill.

Because of the importance in engineering applications of this little-understood phenomenon, an investigation of the mechanics of the process was undertaken by the National Bureau of Standards with the cooperation of the National Advisory Committee for Aeronautics. A system was set up in which several different wide-angle diffusers could be used to connect a duct 18 in. in diameter to a 36-in. duct, and air was drawn through the system by a centrifugal fan at speeds of about 100 ft. per second. By probing along diameters with pitot-static tubes, studies were made of the effects on the flow of fine wire screens (sometimes called wire cloth) placed at various cross sections of the diffusers. While the screens were all of smaller mesh than ordinary insect screen, the porosity to flow was about the same because of the finer wires.

From detailed analysis of data obtained in a 28-deg. diffuser, it became clear that the characteristic action of a screen is to spread a stream and in this way prevent separation of flow from the diffuser walls. However, the screen must be located sufficiently near to the natural separation point to be fully effective. When it is placed at the large end of the diffuser, it generally does not prevent separation and thus does not produce complete filling. Nevertheless, complete filling may always be attained by the use of several screens at properly chosen cross sections of the diffuser. By giving the diffuser walls a special shape, filling may be obtained with a single screen, but this method offers no advantage over the use of several screens in a duct of simple conical form.

Mathematical relations for efficiency—that is, the ratio of available energy leaving the diffuser to that entering—were found for diffusers containing screens. In general, efficiency is low compared to that of an 8-deg. diffuser without screens. Thus, while screens make it possible to spread a stream over a large cross section in a short distance, they do not permit retention of much of its initial kinetic energy.

Flow measurements were also made on multiple-screen arrangements in a 28-deg. and a 90-deg. diffuser to investigate a possible application of diffuser-screen combinations to the general problem of reduction of turbulence in wind tunnels. When damping screens are used upstream of the entrance cone to decrease turbulence, there is ordinarily an appreciable pressure drop across them because of their resistance to flow. However, if the duct area is increased by a wide-

angle diffuser, the pressure drop through the screen may be reduced to negligible proportions, with a significant saving in the power required to drive the tunnel.

FRICTIONAL AND THERMAL BEHAVIOR IN JOURNAL-BEARING LUBRICATION.

The operation of a journal bearing under a steady state of temperature distribution with forced-feed lubrication is dependent upon a number of factors related both to the conditions of operation and to the geometry of the bearing. The relation of these factors to the performance of the bearing is very complex, involving both the rate at which the heat is generated in the bearing and the rate at which it is carried away. In an extensive investigation of these factors at the National Bureau of Standards [1] using a four-bearing friction machine, a method was developed for studying bearing performance through measurements of the combined frictional and thermal behavior in journal-bearing lubrication. These investigations also led to a practical graphical procedure for estimating safe bearing loads.

The work involved operation of bearings of two diameters, in two length-diameter ratios and three clearance-diameter ratios, and at two journal speeds. Three oils, of different viscosity, were used at three oil-inlet temperatures. Particular attention was given to the resultant effects of the combined hydrodynamic and thermodynamic actions involved in bearing operation with forced-feed lubrication.

The four-bearing friction machine, developed and used in former investigations at the National Bureau of Standards, consists essentially of four test bearings on a common shaft. The bearings are mounted in self-aligning ball-bearing swivels which are prevented from rotating by flat springs. The two outer bearings are fastened to the housing while the two inner ones are located in plates that slide in guides. The complete housing floats on the horizontal shaft and acts as a cradle dynamometer. Load is applied by hydraulic jacks under the two inner bearings.

Oil is fed to the bearings through the drilled shaft which has two oil holes at the longitudinal center of each bearing. A motor-driven pump and a relief valve maintain the oil-feed pressure. Bearing temperatures are measured by thermocouples imbedded in the metal at the loaded sides of the bearings.

A study of the frictional-torque data for operation under load indicates that when a bearing is operating at a constant speed, using a given oil at constant oil-inlet temperature and oil-feed pressure, an

---

NOTE: For further technical details of this work, see "Measurements of Combined Frictional and Thermal Behavior in Journal-Bearing Lubrication," by S. A. McKee, H. S. White, and J. F. Swindells, *ASME*, **70**, 409 (1948).

[1] These tests were part of a research program carried out with the cooperation and financial assistance of the National Advisory Committee for Aeronautics.

increase in load produces an approximately proportional increase in frictional-torque. The increase in torque with unit increase in load is influenced chiefly by the viscosity of the oil, the oil-inlet temperature, the oil-feed pressure, the clearance-diameter ratio, and the length-diameter ratio.

The results also indicate that, under these operating conditions, an increase in load causes a proportional increase in the fluidity of the oil in the bearing. For a given oil, oil-inlet temperature, and oil-feed pressure, this increase in fluidity (reciprocal of viscosity) is a function of the speed of the journal, the diameter of the journal, the length-diameter ratio, and the clearance-diameter ratio. Empirical equations have been developed to define this relationship.

The straight-line relationship between fluidity and pressure provides a graphical means for estimating safe loads. The limit for safe operation is based upon a minimum value of a generalized operating variable, ZN/P, where Z is the absolute viscosity of the lubricant, N is the speed of the journal, and P is the pressure on the bearing. The intersection of a line representing a limiting value of this variable with the straight line drawn through the fluidity-pressure data for a given set of conditions gives directly the safe bearing pressure for these conditions.

In analyzing these results it is emphasized that the thermal behavior of a journal bearing operating with forced-feed lubrication is dependent upon a complex relation that involves heat losses by radiation, conduction, and convection, as well as the heat carried away by the oil leaving the bearing. Therefore, the numerical values obtained in any series of tests are dependent upon the heat-dissipation characteristics of the specific apparatus used. In the course of the bearing-research program, however, the operating conditions were such that it was possible to differentiate between the heat carried away by the oil and the heat losses through the apparatus itself.

These data show that under conditions typical of normal high-speed, high-temperature operation practically all of the heat generated in the bearing is carried away by the oil. Accordingly, the straight-line relationship between fluidity and pressure should hold reasonably well in most bearing applications. In these cases considerable information on bearing performance may be obtained by making a few observations of bearing temperature for various known operating conditions. This is of considerable significance since in many bearing installations friction measurements are not practicable.

V.2
194

STRESS-CORROSION TESTS OF HIGH-STRENGTH ALUMINUM ALLOYS.

The current demand for larger, heavier, and faster aircraft has resulted in the development of a number of new high-strength aluminum alloys. As these materials have become available, their resistance to

corrosion has been determined by the National Bureau of Standards, usually at the request of the Armed Services. In connection with the program, several aluminum alloys introduced during the war—namely, the 75S-T, R301-T, R303-T, and the artificially aged 24S-T—were studied to determine their ability to withstand the highly corrosive conditions to which military planes are subjected in tropical areas.

In the course of this investigation, methods and apparatus for accelerated laboratory tests of stressed samples in corrosive solutions were developed and applied [1] by Hugh L. Logan and Harold Hessing of the Bureau staff. Marine-atmosphere exposure tests of the same materials under similar experimental conditions indicate a high degree of correlation between results of the laboratory tests and what may be expected in actual service.

The duralumin type of aluminum-copper-magnesium alloy known as 24S-T was introduced in 1932 and within a decade had largely replaced other aluminum alloys as sheet material for aircraft construction. Although its resistance to corrosion was generally satisfactory, under some conditions it was appreciably attacked upon exposure to a marine atmosphere or sea water. To increase corrosion resistance, it has been used in the form of a "clad" alloy, in which a duralumin sheet is sandwiched between, and integrally bonded to, two thin protective layers of commercially pure aluminum. This, however, results in some sacrifice of tensile strength. As this material has been found to be adequately resistant to corrosion in service, it was used as a standard of comparison in the marine-atmosphere testing of the new alloys.

With the outbreak of the war in 1939, even stronger aluminum alloys became desirable for aircraft use. Efforts were therefore made to develop alloys of greater tensile strength with adequate corrosion resistance. In the R301-T alloy, this result was sought by covering a duralumin-type alloy with an alloy-cladding layer of higher strength than commercially pure aluminum. In the 75S-T and R303-T alloys, tensile properties were improved by the addition of appreciable amounts of zinc. Use was also made of the discovery that elevated-temperature aging of the commercial flat 24S-T alloy results in a marked increase in yield strength.

In the Bureau's investigation of the stress-corrosion resistance of these new materials, standard ASTM flat tensile specimens with $\frac{1}{2}$-in. reduced sections were tested both in the laboratory and in a marine atmosphere under a stress equal to three-fourths of the yield strength. In the laboratory, stressed samples of all alloys were continuously immersed in a sodium chloride-hydrogen peroxide solution (NaCl, 57 g.; 30-per cent H_2O_2, 10 ml.; H_2O, 990 ml.); those containing zinc as an alloying element (R303-T and 75S-T) were also exposed in a boiling

[1] For further technical details see "Stress-Corrosion Tests on High-Strength Aluminum Alloy Sheet," by Hugh L. Logan and Harold Hessing, *J. Research NBS*, **41**, 69 (1948), RP1905.

6-per cent solution of sodium chloride. Unstressed specimens were subjected to the same corrosive conditions in order that the effect of stress in increasing corrosion damage could be evaluated. All clad materials were tested with the cladding intact since the purpose of the tests was to determine the resistance of the commercial alloy as actually used rather than that of the core material itself. Losses in ultimate tensile strength and per cent elongation were taken as criteria of corrosion damage.

Specimens supported vertically and stressed by means of weighted levers were tested in the sodium chloride-hydrogen peroxide solution in cells made of 60-mm. Pyrex cylindrical tubes fitted at each end into slotted bakelite disks. Rubber gaskets placed between the bakelite and the glass, and rubber stoppers molded with rectangular slots slightly smaller than the grip ends of the specimens, completed the cell assemblies. Samples up to 0.064 in. in thickness were kept in the sodium chloride-hydrogen peroxide solution for 24 hours. One-eighth inch specimens were immersed for 72 hr., the solution being renewed at the end of each 24-hr. period. Breaking of a specimen under stress automatically opened a knife switch in the circuit of a solenoid counter actuated once every 6 min. by a clock. The time required for failure of the specimen was thus recorded in units of 1/10 hour. After removal from the solution and cleaning, the specimens were broken in a hydraulic-type tensile testing machine to determine the tensile properties of the corroded material. Metallographic examinations were also made to determine the types of corrosion that had developed. For marine-atmosphere exposure tests, the specimens were supported and stressed in a similar fashion but were left exposed to the atmosphere.

Specimens immersed in boiling sodium chloride solution were stressed by bowing. This was accomplished by a device consisting of a threaded monel rod, insulating washers slotted to hold the ends of the specimen, and two nuts adjacent to the washers. Tension on the bowed specimens was controlled by adjustment of the nuts. The specimens were then placed in wide-mouthed flasks connected to reflux condensers and containing the sodium chloride solution. They remained in the boiling solution for 14 days unless earlier failures occurred. At the end of this time the specimens were removed, cleaned, and broken in tensile tests.

One of the difficulties in stressing specimens by bowing has been the fact that extremely small changes in the length of the chord connecting the ends of the specimen will make appreciable changes in the stress in the outer fiber. An instrument was therefore constructed by means of which the distance from the chord to the outer fiber could be measured to 0.0001 in. and the stress computed much more precisely than by earlier methods. Essentially, this device consists of two fixed pins and, between them, a third removable pin, which is attached to the plunger of

a dial gage. Stresses computed from dial-gage readings differed from stresses obtained from wire strain gages (attached to the concave and convex surfaces of the specimen) by less than 2 per cent at three-fourths of the yield strength.

The results of the investigation indicate that flat, bare 24S-T aluminum alloy sheet aged four hours or longer at 375° F. is not susceptible to stress-corrosion cracking in either the laboratory or marine atmosphere tests, and is at least as resistant to the combined action of stress and corrosion as the commercially heat-treated but unaged material. It was found that aging of a sample of this alloy for three hours at 385° F. produced an increase in yield strength of about 25 per cent above an initial value of approximately 50,000 psi., an increase in tensile strength of about 3 per cent above an initial value of approximately 70,000 psi., and a decrease of about two-thirds in the initial elongation of 17 to 18 per cent. Similar results were obtained when the material was aged for 20 hr. at 350° F., 5 hr. at 375° F., or 1½ hr. at 400° F.

The samples of the other alloys that were tested, with the exception of R301-T, were found adequately resistant to stress-corrosion cracking. The failure of the R301-T samples was the result of the penetration of stress-corrosion into the core material at the machined edges of the relatively narrow (½ in. wide) specimens that were tested. Such damage would probably not be significant in wide sheets, particularly those cut by shearing.

In general, it was apparent that the short-time laboratory tests developed by the National Bureau of Standards give a good indication of the corrosion resistance to be expected of the unclad alloys in a marine atmosphere. However, results of continuous immersion tests on clad material in the laboratory do not necessarily agree with those obtained by exposure in a marine atmosphere.

THE FRANKLIN INSTITUTE.

MUSEUM NOTES.

ATOMIC ENERGY.

The fears of many people who imagine that, by developing nuclear fission for the purpose of making destructive atomic bombs, the United States had seized a bear by the tail, will be set at rest by the exhibition planned for display in the Museum during the months of November, December, and January.

The exhibit, entitled "Atomic Energy is Here for Good," is sponsored by the Brookhaven National Laboratory and Associated Universities, Inc. Scientists have designed the exhibit to help make atomic energy, as Chairman David E. Lilienthal of the U. S. Atomic Energy Commission terms it, "everybody's business." A "world" that is our greatest frontier of science—the nucleus, or the heart of the atom—is brought into focus for the general public in demonstrations, models, displays, panel illustrations, and photomurals.

Featured in the exhibit is a model atomic pile which splits single uranium atoms before the eyes of the spectators. Energy released by this fission process is amplified into visual and sound effects. A tiny capsule of a mixture of radium and beryllium is used in the model to produce the neutrons that pierce the nuclei of uranium atoms in the fission chamber.

The power possibilities of nuclear energy are demonstrated in a model power plant showing how a nuclear reactor, or atomic pile, may some day be employed to generate electric power by means of the great heat release resulting from nuclear fission—heat that may be transformed into steam to drive electric generating machinery.

Other demonstrations and models depict other beneficial uses, stressing the great value of nuclear energy in scientific research and processes relating to the fields of medicine and biology, chemistry, agriculture, metallurgy, and numerous others. A striking feature of this section will be the radioactive flower, growing in soil fertilized by a phosphate containing radioactive phosphorus. A Geiger counter is used to demonstrate the course of "tracer" atoms into the roots, stem, leaves, and flowers of the plant.

A miniature Van de Graaf electrostatic generator, a machine that builds up high charges of static electricity, is one of several scientific instruments demonstrated. When visitors touch the machine when it is accumulating charges up to 125,000 volts, it will literally "make their hair stand on end."

A Wilson cloud chamber shows the paths made by atomic particles in a pressure chamber containing an atmosphere of fog.

To enable the general public to visualize the construction of the atom the exhibit will include a section devoted to basic physics. This portion will analyze the simplest atoms and go on to explain radioactivity, and why the nuclei of the heavy elements, such as uranium, are used in fission processes. Nor is the historical element of the subject neglected.

No pains have been spared to assist visitors in forming a decision of what is to be gained from nuclear energy.

V.2
194

LIBRARY NOTES.

The Committee on Library desires to add to the collections any technical works that members would wish to contribute. Contributions will be gratefully acknowledged and placed in the library. Duplicates received will be transferred to other libraries as gifts of the donor.

Photostat Service. Photostat prints of any material in the collections can be supplied on request. Orders received in the morning are filled the same day. The average cost for a print 9 × 14 inches is thirty-five cents.

The Library and reading room are open on Mondays, Tuesdays, Fridays, and Saturdays from 9 A.M. until 5 P.M., and Wednesdays and Thursdays from 2 P.M. until 10 P.M.

RECENT ADDITIONS.

AGRICULTURE.

NELSON, JOHN A. AND TROUT, G. MALCOLM. Judging Dairy Products. Second Edition. 1948.

ASTRONOMY.

BERNHARD, HUBERT J.; BENNETT, DOROTHY A. AND RICE, HUGH S. New Handbook of the Heavens. Revised Edition. 1948.

BOTANY.

CROCKER, WILLIAM. Growth of Plants. 1948.

CHEMISTRY AND CHEMICAL TECHNOLOGY.

FRANCIS, WILFRED. Boiler House and Power Station Chemistry. Second Edition. 1947.
STEINER, LUKE EBY. Introduction to Chemical Thermodynamics. Second Edition. 1948.

ELECTRICITY AND ELECTRICAL ENGINEERING.

HOLM, RAGNAR. Electric Contacts. 1946.
REED, MYRIE B. Alternating Current Circuit Theory. 1948.
WALKER, R. C. Photoelectric Cells in Industry. 1948.
WILSON, W. The Cathode Ray Oscillograph in Industry. Third Edition. 1948.

ELECTRONICS.

COSSLETT, V. E. The Electron Microscope. 1947.
HATSCHEK, PAUL. Electron-optics. Second Edition. 1948.

ENGINEERING.

EVANS, ULICK R. An Introduction to Metallic Corrosion. 1948.
FINCH, JAMES KIP. Trends in Engineering Education. 1948.

FIRE PROTECTION.

NATIONAL FIRE PROTECTION ASSOCIATION. Crosby-Fiske-Forster Handbook of Fire Protection. Tenth Edition. 1948.

HISTORY.

STEVENS, SYLVESTER K. Pennsylvania; Titan of Industry. 1948.

MANUFACTURE.

ANGUS-BUTTERWORTH, L. M. The Manufacture of Glass. 1948.
PHILLIPS, C. J. Glass, the Miracle Maker. Second Edition. 1948.

MATHEMATICS.

LASSER, J. K. Handbook of Accounting Methods. 1943.
RELTON, F. E. Applied Bessel Functions. 1946.

MECHANICAL ENGINEERING.

OLDENBOURG, RUFUS AND SARTORIUS, H. The Dynamics of Automatic Controls. 1948.

PUTNAM, PALMER COSSLETT. Power from the Wind. 1948.

MEDICINE.

DORLAND, W. A. NEWMAN. American Pocket Medical Dictionary. Seventeenth Edition. 1943.

METALLURGY.

AMERICAN SOCIETY FOR METALS. Metals Handbook. 1948.

PHOTOGRAPHY.

COX, ARTHUR. Optics; the Technique of Definition. Seventh Edition. 1947.
HENNEY, KEITH. Color Photography for the Amateur. Revised Edition. 1948.
MORTENSEN, WILLIAM. Flash in Modern Photography. Second Edition. 1947.

PHYSICS.

COLE, ROBERT H. Underwater Explosions. 1948.
GRIFFITHS, EZER. Methods of Measuring Temperature. Third Edition. 1947.
INGERSOLL, LEONARD ROSE; ZOBEL, OTTO J. AND INGERSOLL, ALFRED C. Heat Conduction. 1948.
MARTIN, L. C. Technical Optics. Volume 1. 1948.
UBBELOHDE, A. R. Time and Thermodynamics. 1947.

PLASTICS.

SOCIETY OF THE PLASTICS INDUSTRY. SPI Handbook. 1947.

RADIO.

SANDEMAN, E. K. Radio Engineering. Volume 1. 1948.
STURLEY, K. R. Radio Receiver Design. Volume 2. 1947.
TERMAN, FREDERICK EMMONS. Radio Engineers Handbook. First Edition. 1943.
TIBBS, CHRISTOPHER S. Frequency Modulation Engineering. 1947.
WILLIAMS, EMRYS. Thermionic Valve Circuits. 1947.

SCIENCE.

CHWISTEK, LEON. The Limits of Science. 1948.
HASLETT, A. W. Science in Transition. 1947.
HOLMSTROM, J. EDWIN. Records and Research in Engineering and Industrial Science. Second Edition. 1947.
STEELMAN, JOHN. Science and Public Policy; a Report to the President. 1947.
WOODBURY, DAVID O. Battlefronts of Industry; Westinghouse in World War II. 1948.

TEXTILES.

DISERENS, LOUIS. Neueste Fortschritte und Verfahren in der Chemischen Technologie der Textilfasern. Two volumes. 1946–1948.
MARSH, J. T. Textile Science. 1948.

PUBLICATIONS RECEIVED.

Introduction to Physics, by Harley Howe. Second ed., 599 pages, 16 × 23 cm., tables, drawings and illustrations. New York, McGraw-Hill Book Co., Inc., 1948. Price, $4.50.

Cathode Ray Tube Displays, edited by Theodore Soller & Others. 746 pages, 16 × 23 cm., tables, drawings and illustrations. New York, McGraw-Hill Book Co., Inc., 1948. Price, $10.00.

The Nature of Patentable Invention, by John E. R. Hayes. Second ed., 187 pages, 15 × 23 cm. Cambridge, Mass., Addison-Wesley Press, Inc., 1948. Price, $5.00.

Design of Machine Elements, by M. F. Spotts. 402 pages, 16 × 23 cm., tables and drawings. New York, Prentice-Hall, Inc., 1948. Price, $6.65.

A CHECK LIST OF FRANKLIN IMPRINTS IN THE LIBRARY OF THE FRANKLIN INSTITUTE.

Compiled by

GEORGE E. PETTENGILL.[1]

The Franklin Institute has recently become indebted to Samuel H. McVitty of Salem, Virginia for a collection of books printed or written by Benjamin Franklin. This generous gift offers the Institute an opportunity to present a list of its Franklin imprints, the number of which has now been brought to sixty. While the collection is not large in proportion to the more than eight hundred titles listed by Campbell,[2] it may be said to be generally representative. There are examples from both the early and late years of Franklin's active printing career, with various highspots in the intervening period, as well as many of the later Franklin and Hall imprints. The most significant lack is any specimen from Franklin's Passy press in France. This is understandable, however, when one considers their comparative scarcity.

Benjamin Franklin began his printing career in Boston, apprenticed to his brother James in 1718. Among the books which issued from the latter's shop during the period of young Benjamin's apprenticeship are to be found the first examples of his work as a printer. The Institute now has several of these James Franklin imprints including Hodder's *Arithmetick* (X9).[3] This is "the first separate English textbook on arithmetic to be printed in America," according to Louis C. Karpinski in his *Bibliography of Mathematical Works Printed in America through 1850.*

Another book of considerable interest is the 1725 edition of William Wollaston's *The Religion of Nature Delineated* (X67), printed by S. Palmer in London. Franklin tells in his *Autobiography* of having worked on this book and of its having influenced him to write and print *A Dissertation on Liberty and Necessity, Pleasure and Pain* (X66 facs.). Only four copies of this pamphlet are known to exist as he destroyed almost all of them because of his subsequent dissatisfaction with the ideas expressed. A facsimile reprint is in the Institute's collection.

The next item of interest is Sewell's *History of the Rise, Increase and Progress of the Christian People called Quakers* (1) published by Samuel Keimer in 1728. Since this book was begun earlier it is probable that Franklin worked on it while he was still associated with Keimer. After he set up his own business with Hugh Meredith, he finished printing approximately the last third of the book for Keimer. Thus this is the first known book on which Franklin worked in his own shop.

Several of the Poor Richard almanacs are included, notably the one for 1758 (607) which was the last written by Franklin and which contains the first printing of "The Speech of Father Abraham." Better known perhaps as "The Way to Wealth," this was a collection of the many proverbs which had appeared in the previous almanacs. Its popularity is attested to by the fact that Paul Leicester Ford in his *Franklin Bibliography* in 1889 listed nearly one hundred and fifty editions. There is also a copy of the last Poor Richard almanac to bear Franklin's name as printer, that for 1766 (723).

Cicero's *Cato Major* of 1744 (290) in the first issue is important because it has been considered by some as the handsomest product of Franklin's press. An apparently unique item is David Evans's *A Short, Plain Help for Parents and Heads of Families*, 2nd edition, Philadelphia, 1740 (145.5). This is not listed in Campbell nor does any other copy appear in the Union Catalog at the Library of Congress. The last year of Franklin's association with the

---

[1] Assistant Librarian, The Franklin Institute Library, Philadelphia, Pa.

[2] Campbell, William J. "The Collection of Franklin Imprints in the Museum of The Curtis Publishing Company, with a Short-Title Check List of All the Books, Pamphlets, Broadsides, &c., known to have been printed by Benjamin Franklin." Philadelphia, Curtis Publishing Co., 1918.

The Curtis Collection is now in the University of Pennsylvania library. Its catalog will be subsequently referred to as Curtis, and the check list will be referred to as Campbell.

[3] Numbers appearing after the titles mentioned in this introduction are those used in the accompanying check list.

printing business he established, 1766, is represented by Letchworth's *A Morning and Evening's Meditation* (728).

To facilitate comparison with Campbell's catalog of the Curtis collection and his check list, the various titles have been listed under the numbers assigned them by Campbell. The Evans item has been placed in its proper order and assigned the previous number with .5 added. In giving descriptions, a short-title entry following Campbell's check list has been used for those items which are fully described in Curtis. For those items not so described, twelve in number, a full collation comparable to that used in the Curtis catalog has been given. Notes have been added of interesting provenance or incomplete copies. All titles are from the McVitty gift unless otherwise indicated.

This is in no sense a supplement to Campbell's work, although it contains supplementary information. It purports to be merely a check list of the holdings of Franklin imprints in the Library of The Franklin Institute.

X2b

PEMBERTON, EBENEZER. A Discourse / Had / By the late Reverend and Learned / Mr. Ebenezer Pemberton, / Previous to the Ordination / Of the Reverend / Mr. Joseph Sewall, / At Boston, September 16. 1713. / Affirming and proving the Validity / of / Presbyterial Ordination. / [Ornament] / Boston: / Printed by J. Franklin, for S. Gerrish, / and Sold at his Shop near the Old Meeting- / House. 1718.

Title, 1 leaf; preface, (2); text, 15. 18 cm.

Generally issued with and as part of the following:

Prince, Thomas. A Sermon Delivered . . . on Wednesday October 1, 1718. At his ordination to the pastoral charge of the South Church in Boston, N.E. . . . To which is added A discourse of the validity of ordination by the hands of Presbyters, previous to Mr. Sewall's on September 16, 1713. By the late Reverend and Learned Mr. Ebenezer Pemberton. . . . Boston: Printed by J. Franklin for S. Gerrish . . . 1718. (8), 76, (4), 15

Presented by Hamilton Vaughan Bail.

V.2
194

X9

HODDER, JAMES. Hodder's / Arithmetick: / Or, That / Necessary Art / Made most Easy. / Being explained in a way familiar to / the Capacity of any that desire to / learn it in a little Time. / By James Hodder, Writing-Master. / The Five and Twentieth Edition, / Revised, Augmented, and above a Thou- / sand Faults Amended, by Henry / Mose, late Servant and Successor / to the Author. / Boston: Printed by J. Franklin, for S. Phillips, / N. Buttolph, B. Elliot, D. Henchman, G. Phil- / lips, J. Elliot, and E. Negus, Booksellers / in Boston, and Sold at their Shops. 1719.

Title, 1 leaf; dedication, (3); to the reader, (4–5); (6–7); contents, (8–10); text, 1–216. 15 cm.

Lacks portrait. Fragment missing from title page affecting border but not text.

X18

CARE, HENRY. English Liberties, / Or The / Free-born Subject's Inheritance; / Containing / Magna Charta, Charta de Foresta, / The Statute De Tallagio non concedendo, / The Habeas Corpus Act, and several o- / ther Statutes; with Comments on each / of them. / Likewise / The Proceedings in Appeals of Murder: Of / Ship-Money; Of Tonnage and Poundage. Of Par- / liaments, and the Qualification and Choice of / Members: Of the Three Estates, and of the Set- / tlement of the Crown by Parliament. / Together with / A short History of the Succession, not by any Here- / ditary Right: Also a Declaration of the Liberties of the / Subject: And of the Oath of Allegiance and Supremacy. / The Petition of Right; with a short but impartial Re- / lation of the Difference between K. Charles I. and the / Long Parliament, concerning the Prerogative of the King, / the Liberties of the Subject, and the Rise of the Civil / Wars. Of Trials by Juries, and of the Qualifications / of Jurors; their Punishment for Misbehaviour, and of / Challenges to them. / Lastly, / Of Justices of the Peace, Coroners, Constables, / Churchwardens, Overseers of the Poor, Surveyors of / the High-ways, &c. With many Law-Cases through- / out the Whole. / Compiled first by Henry Care, and contiued, [sic] with / large

Additions, by W. N. of the Middle-Temple, Esq. / The Fifth Edition. / Boston: Printed by J. Franklin, for N. Buttolph, B. / Eliot, and D. Henchman, and Sold at their Shops. 1721.

Title, 1 leaf; to the reader, (3–4); contents, (5–12); text, 1–288. 17 cm.

A few leaves slightly torn and defective.

X41

WALTER, THOMAS. The sweet Psalmist of Israel. / A / Sermon / Preach'd at the Lecture held in Boston, / by the Society for promoting / Regular & Good Singing, / And for Reforming the / Depravations and Debasements / Our / Psalmody labours under, / In order to introduce the proper and true / Old Way of Singing. / Now published at the Desire of several Ministers / that heard it, and at the Request of the Society / aforesaid. / By Thomas Walter, M.A. / Minister of a Church in Roxbury. / [Three lines of quotation] / Boston: Printed by J. Franklin, for T. Fleet, / in Savage's Court on Cornhill, 1722.

(8), 28 pp. 17 cm. Collation according to Evans 2403. The first and last leaves are missing, possibly a half-title as found in the edition "for S. Gerrish" noted in Curtis, and pp. 27–28.

X66 facs.

[FRANKLIN, BENJAMIN.] A Dissertation on Liberty and Necessity, Pleasure and Pain. London: Printed in the Year 1725.

This is the facsimile reprint by Charles Whittingham, London, listed by Curtis.

X67

[WOLLASTON, WILLIAM.] The Religion of Nature Delineated. London: Printed by S. Palmer, 1725. Third edition.

The collation of this copy varies from that in Curtis, having 219, (11), the additional pages constituting an index.

1

SEWELL, WILLIAM. The History of the Rise, Increase, and Progress of the Quakers. Third edition, corrected. Philadelphia: Samuel Keimer, 1728.

35

(a) ARSCOT, ALEXANDER. Some Considerations Relating to the Present State of the Christian Religion. B. Franklin, 1732.

(b) ——— Some Considerations Relating to the Present State of the Christian Religion. Part II. B. Franklin, 1732.

42 facs.

SAUNDERS, RICHARD. Poor Richard, 1733. B. Franklin [1732]

Facsimile, published by George S. Appleton, Philadelphia [1849]

122

SAUNDERS, RICHARD. Poor Richard, 1739. An Almanack. B. Franklin [1738]

145.5

EVANS, DAVID. A Short, Plain / Help / For / Parents / And / Heads of Families, / To feed their Babes with the / sincere Milk of God's Word. / Being a Short, Plain / Catechism, / Grounded upon God's Word, and agree- / able to the Westminster Assembly's excellent Catechisms. / By David Evans, / A poor Labourer in the Gospel at Tredyffryn in / Pensilvania. / [Four lines of quotations.] / The Second Edition. / Philadelphia: / Printed by B. Franklin, 1740.

Title, 1 leaf; iii–viii; 9–46+. 14 cm.

There is at least 1 leaf missing after p. 46.

Unique copy. Not in Campbell, Evans, or Union Catalog at Library of Congress.

175

(a) WHITEFIELD, GEORGE. A / Continuation / Of the Reverend / Mr. Whitefield's / Journal / During the Time he was detained / in England, by the Embargo. / Vol. II. / [Ornament] / Philadelphia: / Printed and Sold by B. Franklin, in / Market-street, 1740.

Title, 1 leaf; poem, iii–iv; text, 5–63. 14 cm.

(b) ——— A / Continuation / Of the Reverend / Mr. Whitefield's / Journal / From / His Embarking after the Embargo. / To / His Arrival at Savannah in Georgia. / [Ornament] / Philadelphia: / Printed and Sold by B. Franklin, in / Market-street, 1740.

Title, 1 leaf; text, 67–205; Books sold by B. Franklin, (3) pp. 14 cm.

Some pages lack corners affecting the text in a few cases. See note to 176.

176

WHITEFIELD, GEORGE. A / Continuation / Of the Reverend / Mr. Whitefield's / Journal / From / His Embarking after the Embargo. / To / His Arrival at Savannah in Georgia. / [Ornament] / Philadelphia: / Printed and Sold by B. Franklin, in / Market-street, 1740.

Title, 1 leaf; text, 3–145; Books sold by B. Franklin, (3) pp. 14 cm.

Apparently both 175b and 176 lack pp. [3–4] of the ads, for other copies have five pages.

233e

[GRUBER, JOHANN ADAM.] Gründliche An- und aufforderung. B. Franklin, 1742.

235

BECHTEL, JOHANNES. Kurzer Catechismus. B. Franklin, 1742.

237

(a) PENNSYLVANIA. The Charters of the Province of Pensilvania and City of Philadelphia. B. Franklin, 1742.

(b) ——— A Collection of all the Laws of the Province of Pennsylvania Now in Force. B. Franklin, 1742.

(c) ——— An Appendix; Containing a Summary of Such Acts of Assembly as have been formerly in force. B. Franklin, 1742.

Two copies. Copy 1 was presented by Mrs. Arthur Biddle.

256

ZINZENDORFF, NIKOLAUS LUDWIG. B. Ludewigs / Wahrer / Bericht / De dato Germantown den 20sten Febr. 174½, / An seine liebe Teutsche, / Und / Wem es sonst nützlich zu wissen ist, / Wegen Sein und seiner Brüder / Zusammenhanges / Mit Pennsylvania, / Zu Prüfung der Zeit und Umstände ausgefertiget; / Nebst einem P.S. de dato Philadelphia den 5ten Martii; / Und einigen / Unsre Lehre überhaupt und dieses Schriftgen insonderheit / Erläuternden Beylagen. / Philadelphia, / Gedruckt bey Benjamin Franklin.

Title, 1 leaf; 3–26. 23 cm.

258

ZINZENDORFF, NIKOLAUS LUDWIG. Etliche Zu dieser Zeit nicht unnütze Fragen über Einige Schrift-Stellen, Welche . . . B. Franklin, [1742]

289 facs.

[FRANKLIN, BENJAMIN.] A Catalogue of Choice and Valuable Books, Consisting of near 600 Volumes. [B. Franklin, 1744]

"A facsimile of the unique copy in the Curtis Collection of Franklin Imprints, in the University of Pennsylvania Library, with a note by Carl Van Doren. Printed in an edition of 250 copies on the occasion of the meeting of the Bibliographical Society of America in Philadelphia, June 5th, 1948."

Catalogue, p. 1–16; note, 4 pages; colophon, 1 leaf; 1 blank leaf.

Presented by the University of Pennsylvania Library, through Dr. Charles W. David.

290

CICERO, MARCUS TULLIUS. M. T. Cicero's Cato Major. B. Franklin, 1744.

The first issue. In this copy "the upper corner of the title-page is restored and the four last letters of Cicero are pen and ink facsimile."

294

ESTAUGH, JOHN. A Call to the Unfaithful Professors of Truth. B. Franklin, 1744.

"Presentation copy from the author's wife to John Fothergill, the noted English Quaker physician, who acted as an intermediary between Franklin and the Penns in the Pennsylvania troubles. With the following autograph inscription on a front flyleaf: 'Jno Fothergil from E: E: 1744'."

295

[FRANKLIN, BENJAMIN]. An / Account / Of the New Invented / Pennsylvanian / Fire-Places: / Wherein / Their Construction and Manner of / Operation is particularly explained; / Their Advantages above every other / Method of Warming Rooms de- / monstrated; / And all Objections that have been raised against / the Use of Them, answered and obviated. / With Directions for putting them up, and for Using / them to the best Advantage. And a Copper-Plate, / in which the several Parts of the Machine / are exactly laid down, from a Scale of equal Parts. / Philadelphia: / Printed and Sold by B. Franklin. 1744.

Title, 1 page; (1); 1–37; (1) 22 cm.

Folded plate is lacking in this copy.

Signed "T. Godfrey 1744" on the title-page.

An early acquisition of the Library.

312

ARMSTRONG, JOHN. The Art of Preserving Health. B. Franklin, 1745.

P. 87–88 is torn and text damaged.

314

CADWALADER, THOMAS. An Essay on the West India Dry-Gripes. B. Franklin, 1745.

317 a–k

THE CONFESSION of Faith, The Larger and Shorter Catechisms. B. Franklin, 1745.

363

(a) MORGAN, ABEL. Anti-Paedo-Rantism. B. Franklin, 1747.

(b) AN APPENDIX to the Foregoing Work, Written by Another Hand. B. Franklin, 1747.

378

CURRIE, WILLIAM. A Treatise on the Lawfulness of Defensive War. B. Franklin and D. Hall, 1748.

381

FISHER, GEORGE. The American Instructor. Ninth edition. B. Franklin and D. Hall, 1748.

A worn copy affecting text in spots. Three plates wanting.

411 a, b, c,

CHALKLEY, THOMAS. A Collection of the Works of Thomas Chalkley. B. Franklin and D. Hall, 1749.

Paging as given in Curtis is incorrect. Pages ccclxii–ccclxiv are in Roman rather than in Arabic numerals.

Two copies. One contains autograph signature of Chalkley tipped in.

417 facs.

[FRANKLIN, BENJAMIN.] Proposals Relating to the Education of Youth in Pensilvania. Philadelphia: Printed [by B. Franklin and D. Hall] in the year 1749.

"Facsimile reprint, with an introduction by William Pepper. Philadelphia, University of Pennsylvania Press, 1931."

Purchased through the Bloomfield H. Moore Memorial Fund.

447

MORGAN, ABEL. Anti-Paedo-Rantism Defended. B. Franklin and D. Hall, 1750.

458

PENNSYLVANIA. Anno Regni Georgii II. Vigesimo Quarto. General Assembly holden at Philadelphia, Oct. 14, 1750. B. Franklin, 1751.

Lacks p. 151.

460

ARNDT, JOHANN. Des Hocherleuchteten Theologi. B. Francklin und J. Böhm, 1751.
Lacks one preliminary leaf and the last leaf, i.e. pp. 1355–1356. Various other pages are frayed and torn.

475

SAUNDERS, RICHARD. A Pocket Almanac for 1752. B. Franklin and D. Hall [1751]
Interleaved.

478

SHORT, THOMAS. Medicina Britannica: Or A Treatise On Such Physical Plants, As Are Generally to be found in the Fields or Gardens in Great Britain. B. Franklin and D. Hall, 1751.

486

DELAWARE. Laws of the Government of New-Castle, Kent and Sussex, upon Delaware. B. Franklin and D. Hall, 1752.

489

JERMAN, JOHN. The American / Almanack / For the Year of Christian Account / 1753, / Wherein is contained, / The Lunations, Eclipses, Planets Motions and Aspects, / Judgment of the Weather, the Time of the Sun's / and Moon's Rising and Setting, Seven-stars Rising, / Southing and Setting, High-water, Spring tides, / Fairs, Courts, Meetings, and other observable / Days. / Fitted to the Latitude of Forty Degrees North, and a / Meridian of Five Hours West from London, but may / without much Error serve from Newfoundland to South- / Carolina. / By John Jerman, Philom. / [Ten lines of quotation.] / Philadelphia: / Printed by B. Franklin and D. Hall. [1752]
Title, 1 leaf; text, (22) pp. 17 cm.
This is undoubtedly the item listed by Campbell as his 489 although the title is slightly different. Campbell gives Jerman, J. An Almanac for 1753. B. Franklin and D. Hall. [1752] and cites Hildeburn 1261, who locates no copy. The only other copy located is an imperfect one in the Library of Congress.

490

(a) JOHNSON, SAMUEL. Elementa Philosophica. B. Franklin and D. Hall, 1752.
(b) ——— Noetica: or the First Principles of Human Knowledge. B. Franklin and D. Hall, 1752.
(c) ——— Ethica: or the First Principles of Moral Philosophy. Second edition. B. Franklin and D. Hall, 1752.

497

SAUNDERS, RICHARD. Poor Richard improved, for 1753. B. Franklin and D. Hall [1752]

499

(a) PENNSYLVANIA. Votes and Proceedings of the House of Representatives of Pennsylvania, beginning Dec. 4, 1682. Volume the First. In two parts. B. Franklin and D. Hall, 1752.
(b) ——— Votes and Proceedings of the House of Representatives of Pennsylvania. Part the Second. B. Franklin and D. Hall, 1752.
Two copies. See also nos. 515 and 530.

502

FISHER, GEORGE. The American / Instructor: / Or, / Young Man's Best Companion. / Containing, / Spelling, Reading, Writing, and Arithmetick, / in an easier Way than any yet published; and how to qua- / lify any Person for Business, without the Help of a Master. / Instructions to write Variety of Hands, with Copies / both in Prose and Verse. How to write Letters on Bu- / siness or Friendship. Forms of Indentures, Bonds, Bills of / Sale, Receipts, Wills, Leases, Releases, &c. / Also Merchants Accompts, and a short and easy Me- / thod of Shop and Book keeping; with a Description of the / several American Colonies. / Together with the Carpenter's Plain and exact Rule: Shew- / ing how to measure Carpenters, Joyners, Sawyers,

Bricklayers, Plaisterers, / Plumbers, Masons Glasiers, and Painters Work. How to undertake each / Work, and at what Price; the Rates of each Commodity, and the com- / mon Wages of Journeymen; with Gunter's Line, and Coggeshal's De- / scription of the Sliding-Rule. / Likewise the Practical Gauger made Easy; the Art of / Dialling, and how to erect and fix any Dial; with Instructions for Dying, / Colouring, and making Colours. / To which is added, / The Poor Planter's Physician: / With Instructions for Marking on Linnen; how to Pickle and / Preserve; to make divers Sorts of Wine; and many excellent Plaisters, and / Medicines, necessary in all Families. / And also, / Prudent Advice to young Tradesmen and Dealers. / The whole better adapted to these American Colonies, than any / other Book of the like Kind. / By George Fisher, Accomptant. / The Tenth Edition, Revised and Corrected. / Philadelphia: Printed by B. Franklin and / D. Hall, at the New-Printing Office, in Market Street, 1753.

Title, 1 leaf; iii–v; 1–384; five plates. 17 cm.

The fifth plate and various other pages are torn, and partially wanting.

510

SAUNDERS, RICHARD. Poor Richard improved for 1754. B. Franklin and D. Hall [1753]

515

PENNSYLVANIA. Votes and Proceedings of the House of Representatives of Pennsylvania, beginning Oct. 14, 1707. Volume the Second. B. Franklin and D. Hall, 1753.

Two copies. See also nos. 499 and 530.

527

SAUNDERS, RICHARD. Poor Richard improved for 1755. B. Franklin and D. Hall [1754]

530

PENNSYLVANIA. Votes and Proceedings of the House of Representatives of Pennsylvania, beginning Oct. 14, 1726. Volume the Third. B. Franklin and D. Hall, 1754.

Two copies. See also nos. 499 and 515.

541

EVANS, LEWIS. Geographical, Historical, Political, Philosophical, and Mechanical Essays. Philadelphia: Printed by B. Franklin and D. Hall, 1755.

Lacks the folding map.

544

[IBID] Second edition. Philadelphia: Printed by B. Franklin and D. Hall, 1755. And Sold by R. & J. Dodsley, in Pall-Mall, London.

Lacks the folding map.

An early acquisition of the Library.

591

BARCLAY, ROBERT. The Anarchy of the Ranters, And other Libertines. B. Franklin and D. Hall, 1757.

Two copies, the second of which contains Pike's *Epistle* (602) bound at the end.

602

PIKE, JOSEPH. An Epistle to the National Meeting of Friends, in Dublin. B. Franklin and D. Hall, 1757.

Removed from a bound volume. For another copy, see Barclay's *Anarchy of the Ranters* (591).

607

SAUNDERS, RICHARD. Poor Richard improved, being an Almanack for 1758. B. Franklin and D. Hall [1757]

620

HALL, DAVID. A Mite into the Treasury. B. Franklin and D. Hall, 1758.

634

DELL, WILLIAM. The Doctrine of Baptisms, Reduced from its Ancient and Modern Corruptions. Fifth edition. B. Franklin and D. Hall, 1759.

640

RUTTY, JOHN. The Liberty of the Spirit and of the Flesh Distinguished. B. Franklin and D. Hall, 1759.
Two copies.

646

DELL, WILLIAM. The Trial of Spirits, Both in Teachers and Hearers. B. Franklin and D. Hall, 1760.
Top of three leaves cut off affecting "The" on title page and page numbers.

648

LAW, WILLIAM. An Extract from a Treatise Called, The Spirit of Prayer. B. Franklin and D. Hall, 1760.
Two copies, the second bound with two other pamphlets not Franklin imprints.

658

CONTINUATION of the Account of the Pennsylvania Hospital, from May 1, 1754, to May 5, 1761. B. Franklin and D. Hall, 1761.

666

PENNSYLVANIA. Anno Regni Georgii III. Secundo. General Assembly holden at Philadelphia, Oct. 14, 1761–Feb. 17, 1762. B. Franklin, 1762.
Title page is damaged affecting several words, With this is bound 667.

667

[IBID.] And from thence continued to Mar. 26, 1762. B. Franklin, 1762.
Pages 205–210 mutilated and p. 211 wanting. Bound with 666.

673

WOOLMAN, JOHN. Considerations on Keeping Negroes. Part Second. B. Franklin and D. Hall, 1762.
With this has been bound "An Extract from John Woolman's Journal in Manuscript, Concerning the Ministry." n.p., n.d. 7 pp.

680

DUCHÉ, JACOB. The Life and Death of the Righteous. / A / Sermon, / Preached at / Christ-Church, Philadelphia, / On Sunday, February the 13th, 1763, / At the Funeral of / Mr. Evan Morgan. / By Jacob Duché, M.A. / One of the Ministers of the united Churches of / Christ-Church, and St. Peter's, Philadelphia, / and Chaplain to the Right Honourable the Earl / of Stirling. / Philadelphia: / Printed by B. Franklin, and D. Hall. / MDCCLXIII.
Title, 1 leaf; dedication, [iii]–iv, 5–24. 19 cm.

693

LIBRARY COMPANY OF PHILADELPHIA. The Charter, Laws, and Catalogue of Books, of the Library Company of Philadelphia. B. Franklin and D. Hall, 1764.

701

SAUNDERS, RICHARD. Poor Richard improved, being an Almanack for 1765. B. Franklin and D. Hall [1764]
Incomplete, three leaves missing, i.e. pp. [5–6], [33–36]

723

SAUNDERS, RICHARD. Poor Richard improved, being an Almanack for 1766. B. Franklin and D. Hall [1765]
Two copies, the second lacking pages [33–36.]

728

LETCHWORTH, THOMAS. A Morning and Evening's Meditation, Or, A Descant On The Times. A Poem. B. Franklin and D. Hall, 1766.

NOTES FROM THE BIOCHEMICAL RESEARCH FOUNDATION.

Abstract of **Blood Group Substance from Intestinal Mucosa and its Precipitation from Borate.**—CHARLES A. ZITTLE (*Archives of Biochemistry*, **17**: 195, 1948). A polysaccharide fraction from phosphoesterase preparations from calf intestinal mucosa was obtained by precipitation with borate and the relation of this polysaccharide to the blood group substances was demonstrated. Since the relation of the Type 14 *pneumococcus* polysaccharide to blood group substances is well established, Type 14 serum (horse) was used to show this relation. Intestinal mucosa has been shown, therefore, to provide an additional source for the blood group substances. The borate procedure provides a convenient and apparently specific method for the separation of blood group substances from proteins.

CURRENT TOPICS.

Biological Effects of High Energy Radiations.—Study of the biological effects of high-energy radiations, such as 100-million-volt X-rays, will by undertaken by Union College in a research project financed by the Atomic Energy Commission for the Office of Naval Research, President Carter Davidson announced recently. The scientific work will be directed by Dr. Leonard B. Clark, Chairman of the Union College Department of Biology.

The General Electric Company will contribute by making available at its own expense certain resources of its Research Laboratory, including use of the 135-ton betatron for producing X-rays up to 100 million volts, which will be used to radiate the biological specimens.

In announcing the project, President Davidson pointed out that while X-rays of one million volts energy are used in a number of hospitals for cancer therapy, far more penetrating radiations are now available from new machines. Their biological effects, however, are still little known, and it is expected that the new program will shed light on these problems.

Biggest of the radiation generators in the Laboratory, said Dr. C. G. Suits, G-E Vice President in charge of research, is the 100-million-volt betatron. Still more powerful equipment is now under construction. For lower energies there are betatrons and synchrotrons of 80 million, 50 million, and 10 million volts, as well as X-ray generators of more conventional sort for voltages of two million, one million, 400 thousand and still lower figures, down to 1000.

Dr. Clark outlined some of the problems to be attacked. "With X-rays of voltage under one million," he explained, "the effect on living cells seems due to ionization of the atoms of the tissue itself or of the media surrounding the cells. Outer electrons are knocked off these atoms and chemical changes are produced.

"However, at about one million volts, there begins to be evident another effect—the so-called pair formation—in which units of radiation, called photons, are converted by the electric field surrounding the nucleus of the atom into pairs of particles, electrons and positrons. At 100 million volts, almost all the energy absorbed produces this effect, and it is desirable to see whether there is any difference in the biological response produced as compared with low-voltage rays. Also, at such high energies one element may be transmuted into another, and it is barely possible that such transmutations may be biologically important.

"Another thing we want to study," he continued, "is that of possible long-range effects, for they should be known before any application is made to human patients. This can be done by exposing experimental organisms to doses of the radiation too weak to be immediately harmful. Then we can check them perhaps a year later to see if any adverse symptoms have developed."

The contract with the Office of Naval Research calls for three main subjects of investigation.

First is the study of the relations between biological effects and the wavelengths of X-rays from one million to 100 million volts. It is known that the wavelengths of ultraviolet radiation vary in their biological effectiveness, as in preventing rickets. It may be that X-rays from one million to 100 million volts may show similar variations in biological effectiveness.

The second topic assigned is the study of the depth-dose effect of such X-rays in tissues or tissue-like masses of living organisms, as blocks of compressed yeast cells. It is known, for example, that the greater the energy of the X-rays, the smaller is the proportion of rays scattered at the surface and the larger the percentage that penetrate deeply into the body. This brings about a difference in the effects produced at different levels within the tissue, and the distribution of this effect should be known.

The third principal subject concerns a study of the correlation of different particular physiological processes in the same living cells exposed to X-radiation. It is planned to make parallel studies of the effect of X-radiation on a number of physiological processes in the same cell.

R. H. O.

Ceilometers for Army and Navy.—Ninety ceilometers, electronic air safety devices which automatically measure and record the altitudes and densities of clouds, are being produced for the Army and Navy, General Electric's Lighting and Rectifier Divisions have announced.

The ceilometer, already in use by weather bureaus, the Armed Forces, and several civilian air fields, operates equally well by night or day. A super-high-intensity quartz mercury lamp, smaller than a cigarette, mounted at the focal point of a searchlight mirror, sends skyward a beam of light.

Clouds overhead reflect the beam back to earth, and a detector unit, which includes a photo-electric tube pickup, and which is tuned to the same frequency as the light source, automatically analyzes the reflections, and transmits to a recording device a record of cloud heights.

The detector, placed about 1000 ft. from the projector, scans the searchlight beam by swinging slowly from a horizontal to vertical position and back again five times an hour.

Ceilometers make possible an accurate and rapid check of cloud ceilings at all times, expediting landing and takeoff instructions, according to the engineers. Data recorded by the instrument are especially vital to safe flying at airports handling heavy traffic.

One year ago, 125 of the devices were delivered to the Army and Navy for installation at the nation's military fields.

R. H. O.

From 19 Per cent to 90 Per cent.—Typical of the contribution rural electrification makes to the industrial economy of the Nation is that of the 28 rural electric cooperatives in Ohio, says the Rural Electrification Administration. The first Ohio co-op that was financed by REA began operating June 15, 1936, says the U. S. Department of Agriculture.

These 28 Ohio co-ops, all of them financed by loans from the Rural Electrification Administration, own and operate 24,287 miles of line. They serve 96,093 consumers, including 820 rural churches and 260 rural schools.

Collectively, they paid $251,825 in taxes during 1947. They provide employment for 541 persons. They own and operate 171 automobiles and motor trucks.

Since the first loan to an Ohio rural electric co-op was approved by REA in September, 1935, REA has allocated a total of $36,486,272 to its Ohio borrowers. They have repaid $7,901,507 in principal and interest, including $1,167,573 on principal in advance of the date due.

Shortly before the establishment of REA in May, 1935, only 48,048, or 18.8 per cent, of the farms in Ohio were receiving central station electric service. Today, 198,512 Ohio farms, or 90 per cent of the number in the State, receive electric service.

Protect Forests from Fire.—Efforts to prevent fire damage to forest lands probably can never be perfect but the record shows they do greatly reduce the number of fires and hold down the destruction.

Last year's record clearly points out this fact, says the U. S. Department of Agriculture. The figures were compiled by the Forest Service. These show that 543,329,000 acres are now under organized forest fire protection. Unprotected acreage is listed at 111,026,000 acres, about 1 acre out of every 6.

This one-sixth of the acreage had 60 per cent or 3 out of 5 of all the fires on forest land (120,429 out of 200,799). More than seven times as many unprotected acres were burned over, and the damage on the unprotected acres was much larger than it was on the five times as many acres that were under organized protection.

The report emphasizes that 90 per cent of our forest fires are man-caused and therefore preventable.

Radio Signals Sent from Rocket at 72-Mile Height (*Science News Letter*, Vol. 54, No. 6).—A war-developed device, for sending automatic radio signals giving scientific information from a roaring rocket high above the earth, operated successfully at the White Sands Proving Grounds, Las Cruces, New Mexico, in a test just revealed, from an altitude of nearly 7 miles while traveling at over 2800 miles an hour.

The device that provides scientific data from aloft to ground-based recording instruments is known as a telemeter. In this test what is known as the Aerobee telemetering system was used. It has had many successful trials, but this is the first time that this miniature telemetering system has reached an altitude of 71.78 miles above the earth and attained a maximum velocity of 2830 miles an hour.

The information collected and sent to the ground-based recording instruments includes flight characteristics, motor performance and missile aspect, data on cosmic ray intensity, the quality of sunlight above the atmospheric blanket, and changes in the earth's magnetic field. The system has been used to transmit 24 different kinds of information. The records sent are continuous.

The system used in this test was evolved during the war by scientists of Princeton University and of the Applied Physics Laboratory of Johns Hopkins University at Silver Spring, Md. The application to supersonic missiles, those that travel faster than sound, was made at the Applied Physics Laboratory.